Revista Brasileira de Paleontologia, 25(3):189–207, Julho/Setembro 2022
A Journal of the Brazilian Society of Paleontology

doi:10.4072/rbp.2022.3.03

BIOSTRATIGRAPHY AND PALEOENVIRONMENTAL SIGNIFICANCE OF PALEOGENE FORAMINIFERAL ASSEMBLAGES FROM DASHTE ZARI AREA IN HIGH ZAGROS, WEST IRAN

SEYED AHMAD BABAZADEH
Department of Sciences, Payame Noor University, Po. Box 19395-3697, Tehran, Iran.
seyedbabazadeh@yahoo.com, *sababazadeh@pnu.ac.ir* (corresponding author)

DOMINIQUE CLUZEL
Institut de Sciences Exactes et Appliquées, Université de la Nouvelle-Calédonie, BP R4,
98851 Noumea Cedex, New Caledonia. *dominique.cluzel@unc.nc*

ABSTRACT – The Paleogene carbonate deposits of Pabdeh and Jahrum formations are widespread from the northwest (Dashte Zari area) to the southwest of the Shahrekord region in the High Zagros Mountains of Iran and record the lateral and upward transition from open marine into the shallow water environment. The Pabdeh Formation shows a succession of open marine pelagic and hemipelagic limestone, argillaceous limestone, and argillaceous chert. It consists of planktonic wackestone, pellet-planktonic wackestone, mudstone with planktonic foraminifera, and radiolarian siliceous wackestone, which accumulated within the Zagros Foreland Basin. The planktonic foraminifers are assigned to the Late Paleocene–Late Eocene and correspond to subtropical and tropical Zones P4b–E15. The Jahrum Formation is represented by bioclast-bearing limestone and calcarenite. It consists of benthic foraminiferal wackestone, benthic foraminiferal-red algal packstone, and bioclast-intraclast packstone deposited in a shallow platform environment. The Jahrum Formation is inter-fingered in the upper part of the Pabdeh Formation and finally overlies it conformably during the Bartonian–Priabonian. Shallowing and off-lap relationships record basin shrinking, while repeated inter-fingering signals moderate tectonic subsidence. Both formations are disconformably covered by the Late Oligocene–Miocene Asmari Formation.

Keywords: biostratigraphy, Pabdeh Formation, Zagros, Paleogene, Iran.

RESUMO – Os depósitos de carbonato do Paleógeno das formações Pabdeh e Jahrum estão distribuídos do noroeste (área de Dashte Zari) para o sudoeste da região de Shahrekord nas Montanhas High Zagros, Irã e registram a transição lateral e ascendente de um ambiente de mar aberto para um ambiente de águas rasas. A Formação Pabdeh mostra uma sucessão de calcário pelágico e hemipelágico de ambiente marinho aberto, calcário argiloso, e c*hert* argiloso. Consiste em *wackestone* planctônicos, *wackestone pellet*-planctônico, lama com foraminíferos planctônicos, e *wackestone* de radiolários, que se acumulou dentro da Bacia de Zagros. Os foraminíferos planctônicos são atribuídos ao Paleoceno Superior–Eoceno Superior e correspondem às zonas subtropicais e tropicais P4b-E15. A Formação Jahrum é representada por calcário bioclástico e calcarenito. Consiste em *wackestone* de foraminíferos bentônicos, *packstone* de algas vermelhas-foraminíferos bentônicos, e *packstone* de bioclastos-intraclastos depositados em um ambiente de plataforma rasa. A Formação Jahrum é interdigitada na parte superior da Formação Pabdeh e finalmente a sobrepõe concordantemente durante o Bartoniano–Priaboniano. Relações rasas e *off-lap* registram encolhimento da bacia, enquanto repetidas interdigitações sinalizam subsidência tectônica moderada. Ambas as formações são cobertas de forma discordante pela Formação Asmari do Oligoceno Superior–Mioceno.

Palavras-chave: bioestratigrafia, Formação Pabdeh, Zagros, Paleógeno, Irã.

INTRODUCTION

The Iranian ranges long have been considered part of the Alpine-Himalayan System (Stöcklin, 1968, 1977; Sengor *et al*., 1988; Babazadeh, 2003). This orogenic belt, which resulted from the closure of the Mesozoic Neo-Tethys, extends from western Europe (west Neo-Tethys) to Tibet passing through Turkey, Iran, Afghanistan (central Neo-Tethys), and possibly continues to Burma and Indonesia (east Neo-Tethys) (Sengor *et al*., 1988; Ahmad *et al*., 2014). Multiple continental blocks were amalgamated and are now separated by ophiolitic complexes (Stöcklin, 1977). During the Late Cretaceous, northeastward subduction beneath the Iranian subplate led to the closure of the central Neo-Tethys and ophiolite obduction onto the margin of the Afro-Arabian Plate (Stöcklin, 1977; Berberian & King, 1981; Davoodzadeh & Schmidt, 1981; Stoneley, 1981; Berberian, 1995; Alavi, 2004). Continent-continent collision starting in the Cenozoic led to the formation of the Zagros fold-and-thrust belt and associated Zagros Foreland Basin, in which Late Cretaceous to Miocene sediments accumulated (Figure 1A). During the Paleocene and Eocene, the Pabdeh Formation (pelagic marls and argillaceous limestones) and the Jahrum Formation (shallow marine carbonates) were deposited in the middle part and on both sides of the Zagros Basin axis respectively (Motiei, 1993). During the Oligocene–Miocene this basin narrowed gradually and the Asmari Formation, which consists of dolomitized carbonate ramp limestones, calcareous sandstones, and evaporites was deposited (*e.g*., Ehrenberg *et al*., 2007). In the study area, the lower contact of the Pabdeh Formation with the underlying Upper Cretaceous Gurpi Formation is faulted. The Jahrum Formation is inter-fingered in the upper part of the Pabdeh Formation and overlaps it at its top. In the southwestern part of the Zagros Basin, the Asmari Formation overlies the Pabdeh Formation, whereas in the Fars and Lurestan regions it covers the Jahrum and Shahbazan formations. Although the lower part of the Asmari Formation is locally inter-fingered with the Pabdeh Formation, its upper part extends over the entire Zagros Basin. The Zagros Mountains include the High Zagros (Internal Zagros), Folded Zagros (Outer Zagros), and Khuzestan plain. In the High Zagros, the Shahrekord region of Chahar-Mahale Bakhtiari Province is subdivided into northeast (Z1), central (Z2), and southwest (Z3) fault-bounded zones. The Central Zone (Z2) is located between the Saman-Fereidoon Shahr thrust (F1) and the Bazoft thrust (F3) (Zahedi & Rahmati Ilkhechi, 2006). This zone is divided into two smaller sub-zones z2a and Z2b, which are located in the Shahrekord region (Figure 1B). It consists of the Upper Cretaceous to Paleogene Gurpi, Jahrum, Pabdeh, and Asmari formations. The studied Dashte Zari section (32°25'N; 50°20'E) is located in the sub-zone Z2b of the structural division of northwest Shahrekord city (Figure 1C).

In the study area, the Pabdeh Formation is subdivided into Lower and Upper units and consists of pelagic carbonate and siliceous sediments, which include a succession of gray thin-bedded limestone, cream argillaceous limestone, and argillaceous chert. In contrast, the Jahrum Formation is composed of shallow marine grey to cream bioclastic limestone and calcarenite. The Pabdeh Formation passes upwards and laterally into the Jahrum Formation and up section (Figure 2). James & Wynd (1965) and Adams & Bourgeois (1967) were pioneers in the study of microfossils and microfacies of the Paleogene carbonate deposits in the Zagros Basin. They established the benthic foraminiferal biozonation of the Jahrum Formation in the southwest and west Iran. Basic works on the Paleogene biostratigraphy of benthic foraminifera in the High Zagros Basin and other basins along the southwestern margin of Iran focused mostly on microfacies and macrofossils (Kalantari, 1975, 1986; Rahaghi, 1976, 1978, 1980, 1983; Stöcklin & Setudehnia, 1991; Khatibi Mehr & Moalemi, 2009; Babazadeh *et al*., 2015). The foraminiferal assemblage zones of the Jahrum Formation and its equivalents were reported by a few researchers such as James & Wynd (1965) and Hottinger (2007). On the other hand, the Pabdeh Formation was analyzed by several researchers (Kalantari, 1986; Babazadeh *et al*., 2010; Daneshian *et al*., 2015; Chegni *et al*., 2016; Moradian & Baghbani, 2016; Moradian *et al*., 2017; Hadavandkhani *et al*., 2018) based on biofacies and stratigraphy of samples from outcrops of the folded Zagros and Khuzestan plain, whereas the analysis of biostratigraphic zonation of planktonic foraminifera is extensively conducted for the first time in the High Zagros of Chahar-Mahale Bakhtiari Province. The purpose of this study is: (i) to document the planktonic and benthic foraminiferal fauna, and (ii) to introduce the Paleogene foraminiferal biozonations.

MATERIAL AND METHODS

A total of 111 samples of Pabdeh and Jahrum formations from the Dashte Zari section are used in this study. Most of the diagnostic criteria such as the size of the test, the shape of chambers, the thickness of the test, and the number of keels can be recognized in axial and sub-axial sections in thin sections. The thin sections of the specimen samples were prepared in Payame Noor University Laboratory. The Paleogene planktonic foraminiferal zonations were established by many researchers: Toumarkine & Lutertacher (1985); Berggren *et al*. (1995); Olsson *et al*. (1999); Berggren & Pearson (2005), and Wade *et al*. (2011). Besides, the calibration of the first occurrence (**FO**) and last occurrence (**LO**) data of planktonic species is based on Berggren *et al*. (1995) and Berggren & Pearson (2005). The identification of Paleogene planktonic foraminiferal species in thin sections is carried out based on the following publications: Postuma (1971); Wernli *et al*. (1997); Konijnenburg *et al*. (1998); Olsson *et al.* (1999); Premoli Silva *et al*. (2003); Babazadeh *et al*. (2010); Daneshian *et al*. (2015); Sari (2017); Sarigul *et al*. (2017), and pforams@mikrotax. The species identification of benthic foraminifera was made by reference mainly to Ellis & Messina (1940); Le Calvez (1949); Cole & Gravell (1952); Hanzawa (1957); Rahaghi (1980); Loeblich & Tappan (1987); Ozgen (2000); Sirel (2003, 2009); Ozcan *et al*., (2007); Hottinger (2007); Serra Kiel *et al*., (2007, 2016), and Hayward *et al.* (2021). A brief evaluation of the depositional setting is also presented following Murray (1991), Hottinger (1983, 1997), and Flügel (1982, 2004). The biozonal schemes of Berggren *et al*. (1995) and Berggren & Pearson (2005) were correlated with relevant data levels of species found in the study area.

STRATIGRAPHY

The excellent exposures of Paleogene carbonate sedimentary rocks of the High Zagros Basin of southwest and west Iran have allowed detailed stratigraphical and micropaleontological investigations of these rocks. The Paleocene–Eocene marine deposits of the Pabdeh and Jahrum formations in the Dashte Zari section contain planktonic

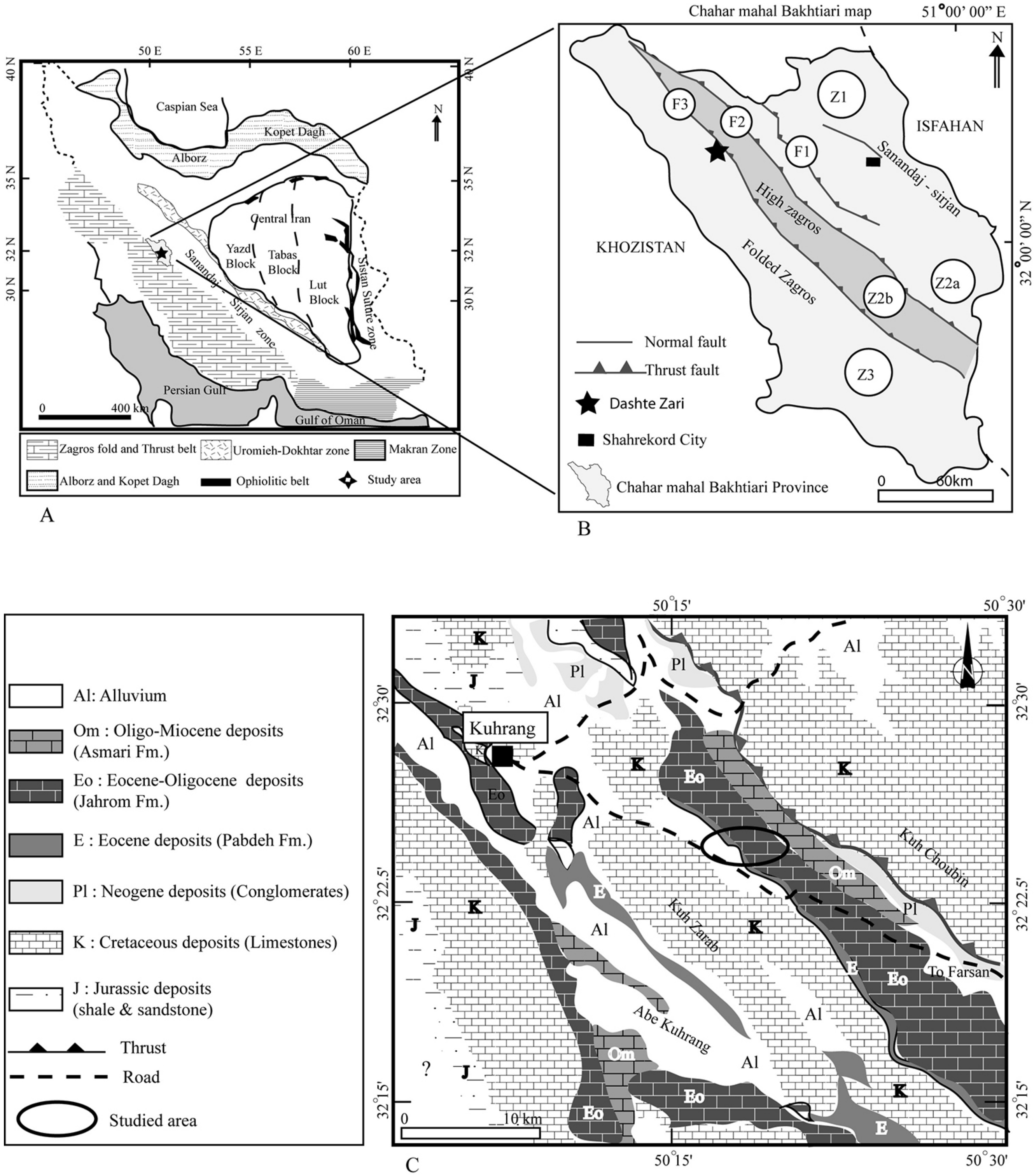

Figure 1. **A**, Iran map showing the several sedimentary basin zones (Zagros and Alborz Mountains, Kopet Dagh, etc.) (Alavi, 2004). **B**, the zonal subdivisions of High Zagros in Chaharmahal Bakhtiari Province (Zahedi & Rahmati Ilkhechi, 2006). **C**, location of the study area (Dashte Zari area) in Shahrekord geological map (1:250.000).

and larger benthic foraminifera, which provide the basis for regional biostratigraphy. Due to the presence of faults and discontinuous outcrops of Paleogene successions in the Shahrekord region, planktonic biostratigraphic research was not conducted until today.

BIOSTRATIGRAPHY

The planktonic foraminiferal zonations of Berggren *et al*. (1995, 2006), Berggren & Pearson (2005), Wade *et al*. (2011), and the benthic foraminiferal zonations of Serra-Kiel

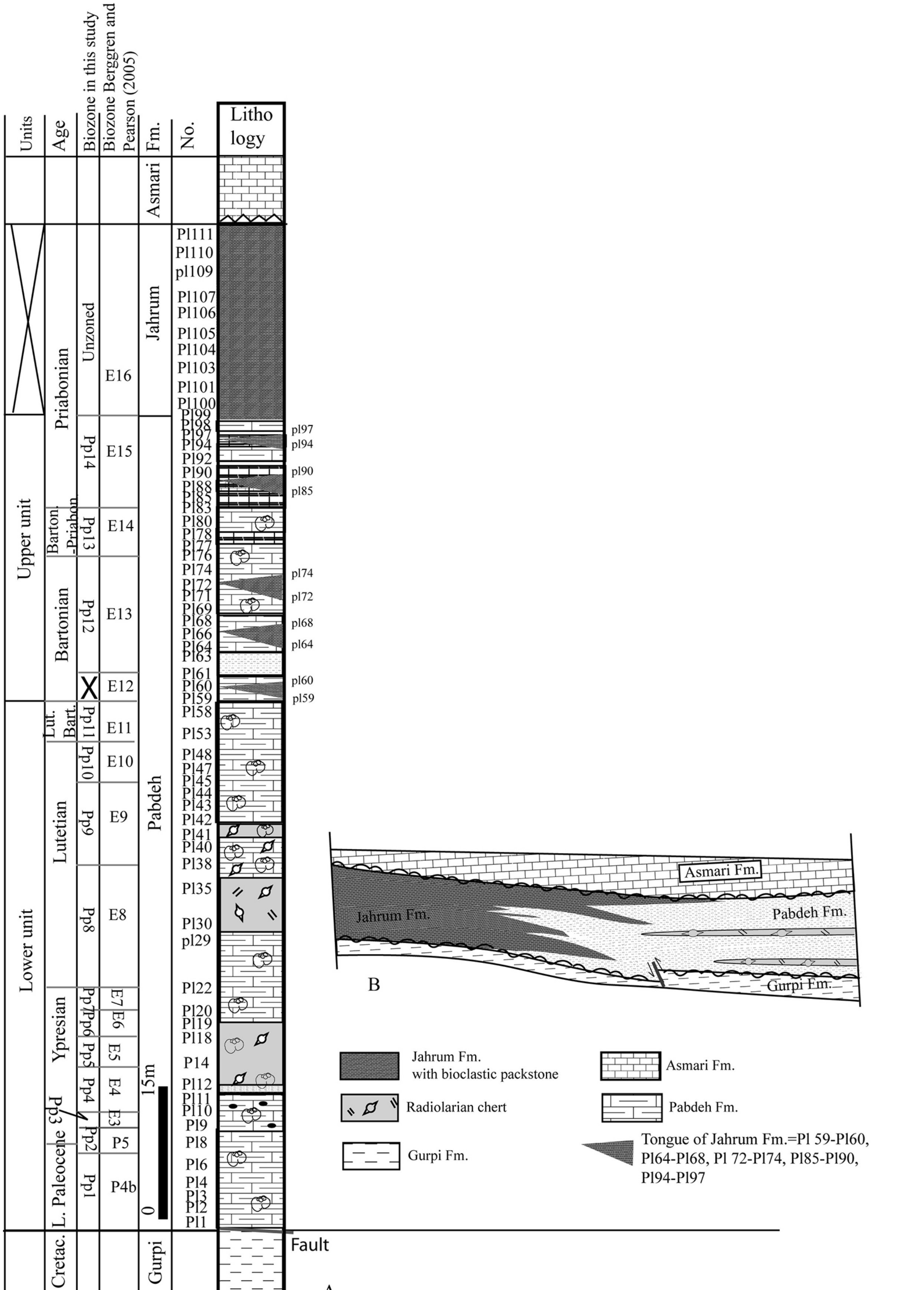

Figure 2. A, distribution of lithofacies of Pabdeh and Jahrum formations on the stratigraphic section. **B**, lateral lithofacies changes between both formations (Pabdeh and Jahrum) in the study area.

et al. (1998) and Hottinger (2007) are adopted for comparison and interpretation. The planktonic and benthic foraminiferal assemblages from hemipelagic and neritic successions of the High Zagros provide the first published biostratigraphic data on this area. A total of 46 planktonic foraminiferal species belonging to 14 different genera, and 19 benthic foraminiferal species belonging to 17 different genera have been identified and led to the recognition of 14 planktonic biozones and three benthic associations respectively. The columnar stratigraphic section of the studied area is summarized in Figure 3, which shows the distribution of selected taxa of planktonic and benthic foraminifera. In general, the stratigraphic range of selected Paleogene planktonic and benthic foraminifera is illustrated in Figures 4 and 5. The planktonic foraminiferal biozonations enable to correlate with other biostratigraphic scales and to make more precise age determination (Figure 6).

Pabdeh Formation

The planktonic foraminiferal biozones are as follows:

Pp1: *Acarinina subsphaerica* Zone (TRZ)
TRZ: Total Range Zone

Estimated age. 59.2–56.5 Ma (Cande & Kent, 1995); 60.0–57.3 Ma (Luterbacher *et al*., 2004); Middle–Late Paleocene (Wade *et al*., 2011).

This zone, characterized by the total range zone of *Acarinina subsphaerica* (Subbotina) has a thickness of 9 m (bed Pl 1 to bed Pl 7). It is equivalent to subzone P4a (*Globanomalina pseudomenardii-Acarinina subsphaerica* CRSZ), subzone P4b (*A. subsphaerica–A. soldadensis* ISZ) of Berggren *et al*. (1995), and subzone P4b (*A. subsphaerica* PRSZ) of Berggren & Pearson (2005) and Wade *et al*. (2011), thereby indicating Selandian to Thanetian age for the lowermost part of the Pabdeh Formation in the study area. The associated planktonic fauna is *Acarinina decepta* (Martin), *Acarinina mckannai* (White), and *Acarinina* cf. *nitida* (Martin). The associated foraminiferal taxa are well represented throughout the Late Paleocene to Early Eocene. This zone is assigned to the late Selandian–Thanetian in the study area.

Pp2: *Morozovella velascoensis* Zone (PRZ)
PRZ: Partial Range Zone

Estimated age. 55.9–55.5 Ma (Cande & Kent, 1995); 56.7–55.8 Ma (Luterbacher *et al*., 2004); Late Paleocene (Wade *et al*., 2011).

The biostratigraphic interval is characterized by the partial range of the nominate taxon between the LO (Last Occurrence) of *Acarinina mckannai* (White) and the first occurrence (FO) of *Morozovella marginodentata* (Subbotina). This zone has a thickness of 3.5 m and only appears on level Pl 8. It is comparable to Zone P4c (*A. soldadoensis–Gl. pseudomenardii* ISZ); Zone P5 (*M. velascoensis* IZ) of Berggren *et al*. (1995), Zone E1 (*A. sibaiyaensis* LOZ) and Zone E2 (*P. wilcoxensis–M. velascoensis* CRZ) of Berggren & Pearson (2005), thereby indicating Late Paleocene (Thanetian) to Early Eocene age in this study. This zone also contains *Acarinina* cf. *nitida* (Martin).

Pp3: *Morozovella marginodentata–Morozovella formosa* Zone (IZ)
IZ: Interval Zone

Estimated age. 54.5–54.0 Ma (Cande & Kent, 1995); 54.9–54.4 Ma (Luterbacher *et al*., 2004); Early Eocene (Early Ypresian) (Wade *et al*., 2011).

This zone, marked by the FO of *Morozovella marginodentata* (Subbotina) and the FO of *Morozovella formosa* (Bolli), extends over a thickness of 2.5 m (bed Pl 9 to bed Pl 10). It corresponds to the *Globorotalia edgari* Zone of Premoli Silva & Bolli (1973) (in part), the Zone P6a (*Morozovella velascoensis–M. formosa*/*–M. lensiformis* ISZ) of Berggren *et al*. (1995), and the Zone E3 (*Morozovella marginodentata* PRZ) of Berggren & Pearson (2005) and Wade *et al*. (2011). The associated planktonic foraminifera of this biozone are *Morozovella edgari* (Premoli Silva & Bolli), *Morozovella velascoensis* (Cushman), *Morozovella acuta* (Toulmin), *Morozovella marginodentata* (Subbotina) and *Acarinina nitida* (Martin). The stratigraphic range of this zone is Early Eocene (early Ypresian).

Pp4: *Morozovella formosa–Guembelitrioides lozanoi* Zone (IZ)

Estimated age. 54.0–52.3 Ma (Cande & Kent, 1995); 54.4–52.3 Ma (Luterbacher *et al*., 2004); Early Eocene (Ypresian) (Wade *et al*., 2011).

The biostratigraphic interval is characterized by the FO of *Morozovella formosa* (Bolli) and FO of *Guembelitrioides lozanoi* (Colom). This zone is 5 m thick (bed Pl 10 to bed Pl 14). It corresponds to the Zone P6b (*M. aragonensis-M. formosa*) of Berggren *et al*. (1995) and Zone E4 (*Morozovella formosa* LOZ) of Berggren & Pearson (2005) and Wade *et al*. (2011). The associated planktonic foraminifera of this biozone are *Acarinina* cf. *A. nitida* (Martin), *Igorina (Pearsonites) broedermanni* (Cushman & Bermudez), *Morozovella velascoensis* (Cushman), *Morozovella marginodentata* (Subbotina), and *Morozovella subbotinae* (Morozova). This associated species ranges within the Early Eocene (Ypresian) age.

Pp5: *Guembelitrioides lozanoi–Acarinina pentacamerata* (IZ)

Estimated age. 52.3–50.8 Ma (Cande & Kent, 1995 and Luterbacher *et al*., 2004); Early Eocene (Ypresian) (Wade *et al*., 2011).

This zone, characterized by the FO of *Guembelitrioides lozanoi* (Colom) and the FO of *Acarinina pentacamerata* (Subbotina), extends over a thickness of 2.8 m (Pl 14 to Pl 18). This biozone can be equivalent to the Zone P7 (*M. aragonensis*/*–M. formosa*) and Zone E5 (*M. aragonensis*/*–M.*

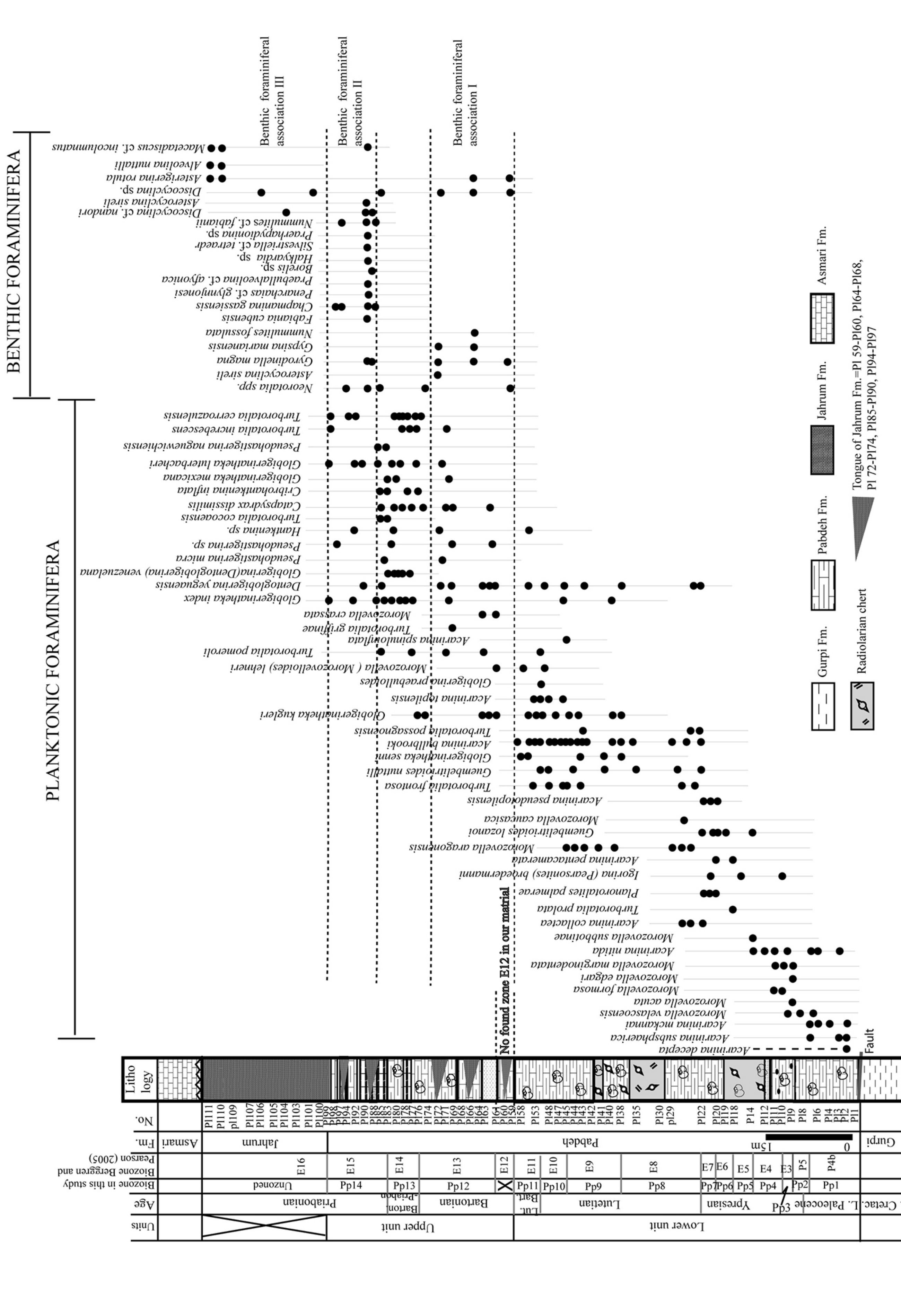

Figure 3. Distribution of selected planktonic and benthic foraminifera on the stratigraphic column.

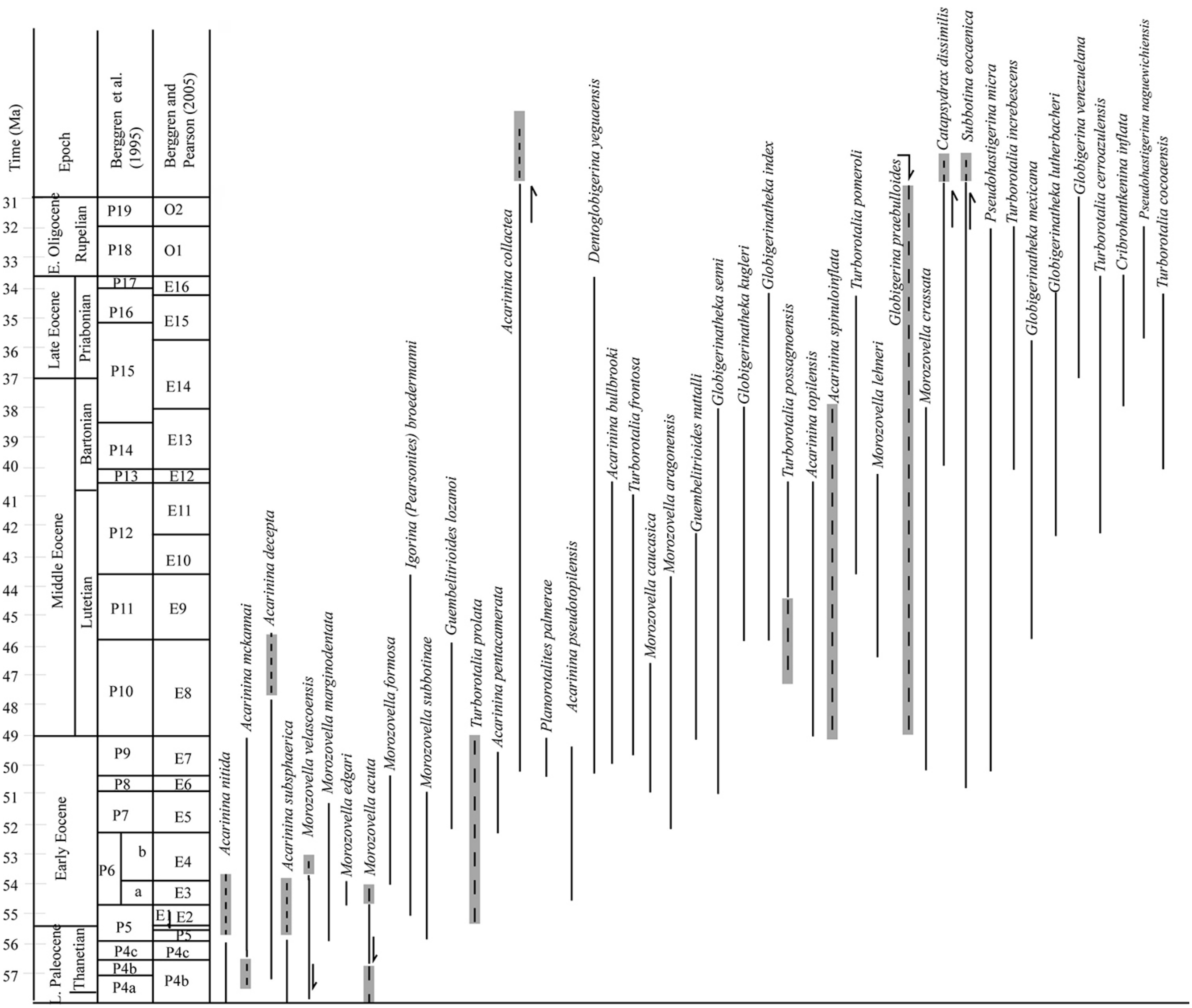

Figure 4. Stratigraphic range of selected Paleogene planktonic foraminifera based on Olsson *et al*. (1999); Berggren *et al*. (1995, 2006); Berggren & Pearson (2005); pforams@mikrotax and the study area.

subbotinae CRZ) of Berggren & Pearson (2005) and Wade *et al*. (2011). The associated fauna of this biozone consists of *Igorina broedermanni* (Cushman & Bermudez), *Morozovella subbotinae* (Morozova), *Guembelitrioides lozanoi* (Colom), and Radiolaria and extends throughout the Early Eocene (Ypresian).

Remark. The first radiolarian association occurs in the interval from bed 12 to bed 18.

Pp6: *Acarinina pentacamerata–Planorotalites palmerae* Zone (IZ)

Estimated age. 50.8–50.4 Ma (Cande & Kent, 1995); 50.8–50.3 Ma (Luterbacher *et al*., 2004); Early Eocene (Ypresian) (Wade *et al*., 2011).

This zone, marked by the FO of *Acarinina pentacamerata* (Subbotina) and the FO of *Planorotalites palmerae* Cushman & Bermudez, is 2.5 m thick (bed Pl 18 to bed Pl 20). It is equivalent to Zone P8 *(M. aragonensis* PRZ) of Berggren *et al*. (1995) and Zone E6 *(A. pentacamerata* PRZ) of Berggren & Pearson (2005) and Wade *et al*. (2011). This zone also contains *Guembelitrioides lozanoi* (Colom) and *Turborotalia prolata* (Belfoed). The stratigraphic range of this zone is assigned to the Early Eocene (early Ypresian).

Pp7: *Planorotalites palmerae–Guembelitrioides nuttalli* Zone (IZ)

Guembelitrioides nuttalli is synonymous with *Globigerinoides higginsi*

Estimated age. 50.4–49.0 Ma (Cande & Kent, 1995); 50.3–48.6 Ma (Luterbacher *et al*., 2004); Early Eocene (late Ypresian) (Wade *et al*., 2011).

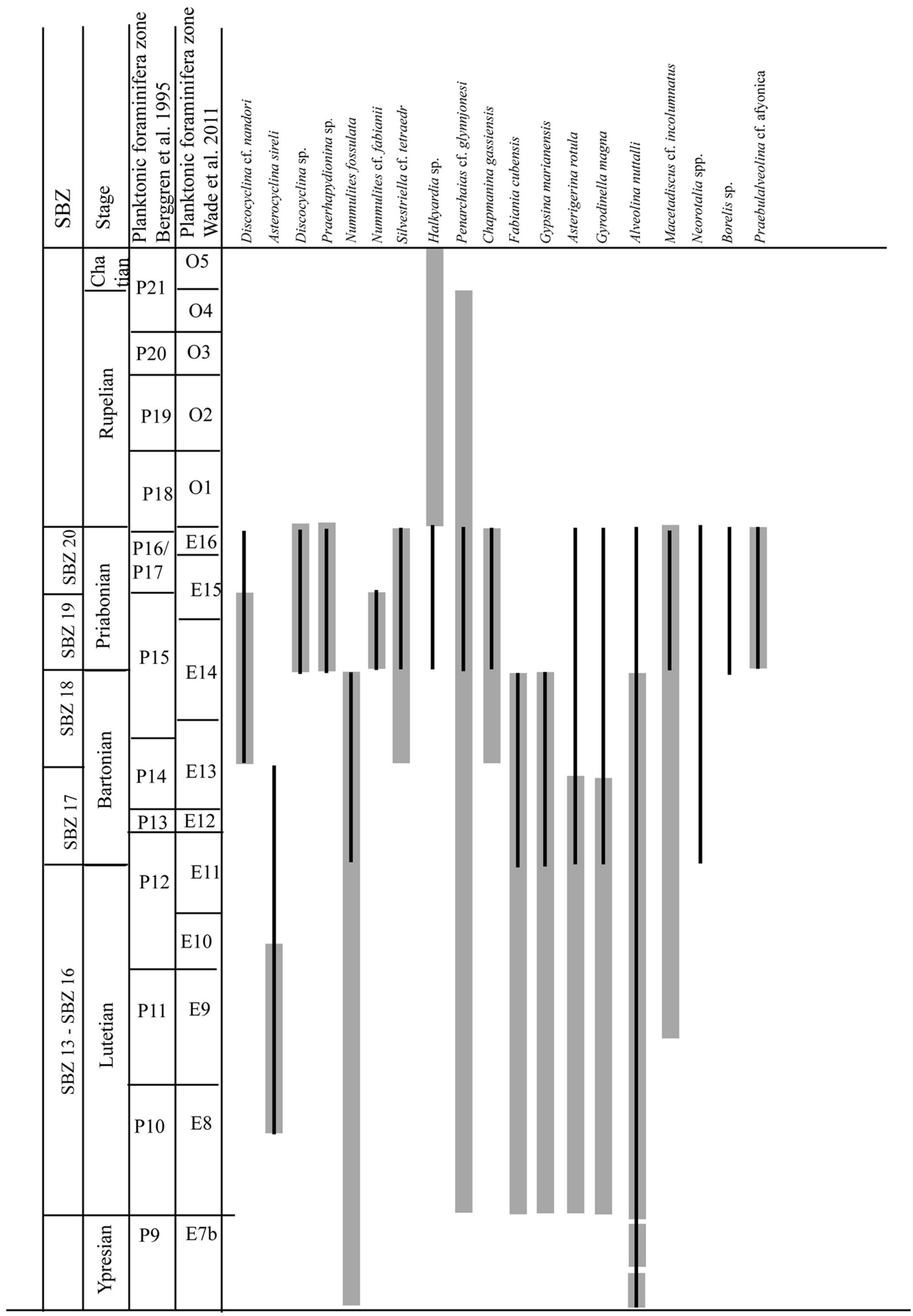

Figure 5. Stratigraphic range of selected Paleogene larger benthic foraminifera, black lines indicate the occurrences of the species in the study area, and pale grey bars show known global ranges of genera (Le Calvez, 1949; Cole & Gravell, 1952; Hanzawa, 1957; Ozgen, 2000; Ozcan *et al*., 2007; Hayward *et al*., 2021 and Serra-Kiel *et al*., 1998, 2007, 2016).

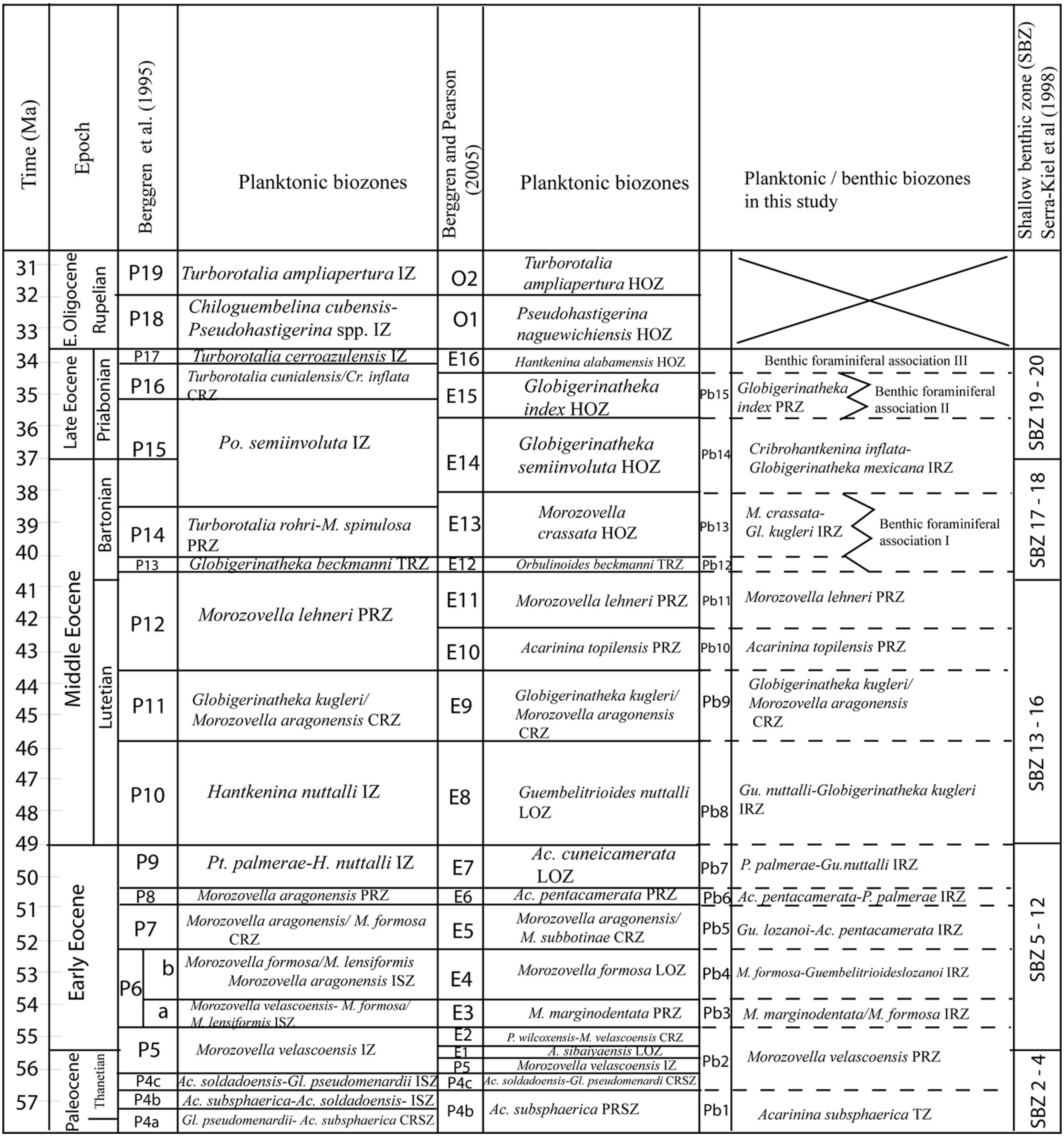

Figure 6. Correlation chart of Planktonic and benthic foraminiferal assemblages in the study area and published biostratigraphic data (Berggren *et al*., 1995; Berggren & Pearson, 2005; Serra-Kiel *et al*., 1998). **Abbreviations: Ac**, *Acarinina*; **Gl**: *Globigerinatheka*; **Gu**, *Guembelitrioides*; **M**, *Morozovella*; **P**, *Planorotalites*; **Ps**, *Pseudohastigerina*.

This zone, characterized by the FO of *Planorotalites palmerae* Cushman & Bermudez and the FO of *Guembelitrioides nuttalli* (Hamilton), is 2.3 m thick (bed Pl 20 to bed Pl 22). It corresponds to the Zone P9 (*P. palmerae–G. nuttalli* IZ) of Berggren *et al*. (1995); Zone E7 (*Acarinina cuneicamerata* LOZ) of Berggren & Pearson (2005) and Zone E7a (*Acarinina cuneicamerata* LOSZ) of Wade *et al*. (2011). This zone also contains *Acarinina collactea* (Finaly), *Acarinina pentacamerata* (Subbotina), *Guembelitrioides lozanoi* (Colom), *Planorotalites palmerae* Cushman & Bermudez, *Igorina (pearsonites) broedermanni* (Cushman & Bermudez) and *Acarinina pseudotopilensis* Subbotina. This species association is assigned to the late Early Eocene (late Ypresian).

Pp8: *Guembelitrioides nuttalli–Globigerinatheka kugleri* Zone (IZ)

Estimated age. 46.4–44.4 Ma (Cande & Kent, 1995); 45.5–43.4 Ma (Luterbacher *et al*., 2004); Middle Eocene (Wade *et al*., 2011).

This zone, marked by FO of *Guembelitrioides nuttalli* (Hamilton) and FO of *Globigerinatheka kugleri* (Bolli, Loeblich & Tappan), is 14 m thick (bed Pl 22 to bed Pl 38). It corresponds to the Zone P10 (*Hantkenina nuttalli* IZ) of Berggren *et al*. (1995), Zone E8 (*G. nuttalli* LOZ) of Berggren & Pearson (2005) and Wade *et al*. (2011). The associated fauna consists of *Dentoglobigerina yeguaensis* (Weinzierl & Applin), *Guembelitrioides lozanoi* (Colom), *Truncorotaloides* sp., *Acarinina bullbrooki* (Bolli), *Turborotalia frontosa* (Subbotina), *Morozovella caucasica* (Glaessner) and *Morozovella aragonensis* (Nuttall). This zone is assigned to the Middle Eocene (early Lutetian).

Remark. The second radiolarian association occurs in the interval from bed Pl 30 to bed Pl 35.

Pp9: *Globigerinatheka kugleri–Morozovella aragonensis* Zone (CRZ)
CRZ: Concurrent Range Zone

Estimated age. 44.4–43.6 Ma (Cande & Kent, 1995); 43.4–42.6 Ma (Luterbacher *et al*., 2004); middle Eocene (Wade *et al*., 2011).

This zone is characterized by the concurrent range of the nominate taxa between the FO of *Globigerinatheka kugleri* (Bolli, Loeblich & Tappan) and the LO (last occurrence) of *Morozovella aragonensis* (Nuttall), which is 8.5 m thick (bed Pl 38 to bed Pl 45). This zone is equivalent to P11 (*G. kugleri–M. aragonensis* CRZ) of Berggren *et al*. (1995) and Zone E9 (*G. kugleri-M. aragonensis* CRZ) of Berggren & Pearson (2005) and Wade *et al*. (2011). This zone also contains *Guembelitrioides nuttalli* (Hamilton), *Acarinina bullbrooki* (Bolli), *Dentoglobigerina yeguaensis* (Weinzierl & Applin), *Globigerinatheka senni* (Beckmann), *Globigerinatheka kugleri* (Bolli, Loeblich & Tappan), *Globigerinatheka index* (Finlay), *Turborotalia possagnoensis* (Toumarkine & Bolli), *Turborotalia frontosa* (Subbotina) and *Morozovella aragonensis* (Nuttall). This association corresponds to the Middle Eocene (Middle Lutetian).

Remark. The third radiolarian association occurs in the interval from bed Pl 41 to bed Pl 42.

Pp10: *Acarinina topilensis* Zone (PRZ)
(PRZ): Partial Range Zone

Estimated age. 43.6–42.3 Ma (Cande & Kent, 1995); 42.6–41.4 Ma (Luterbacher *et al*., 2004); Middle Eocene (Wade *et al*., 2011).

This zone is defined by the LO of *Morozovella aragonensis* (Nuttall) and the LO of *Guembelitrioides nuttalli* (Hamilton), which is 5 m thick (bed Pl 46 to bed Pl 51). It is equivalent to the lower part of P12 (*M. lehneri* PRZ) of Berggren *et al*. (1995) and Zone E10 (*A. topilensis* PRZ) of Berggren & Pearson (2005) and of Wade *et al*. (2011). This zone also contains *Acarinina spinuloinflata* (Bandy), *Guembelitrioides nuttalli* (Hamilton), *Globigerinatheka index* (Finlay), *Acarinina topilensis* (Cushman), *Acarinina bullbrooki* (Bolli), *Turborotalia frontosa* (Subbotina), *Turborotalia pomeroli* (Toumarkine & Bolli), *Dentoglobigerina yeguaensis* (Weinzierl & Applin), *Morozovella* (*Morozovelloides*) *lehneri* (Cushman & Jarvis), *Globigerina praebulloides* Blow, and *Globigerinatheka kugleri* (Bolli, Loeblich & Tappan). Based on planktonic foraminifera, this level can be assigned to the Middle Eocene (middle Lutetian).

Pp11: *Morozovelloides lehneri*
Partial–Range Zone (PRZ)

Estimated age. 42.3–40.5 Ma (as per Cande & Kent, 1995); 41.4–39.8 Ma (as per Luterbacher *et al*., 2004); middle Eocene (Lutetian-Bartonian) (Wade *et al*., 2011).

This zone, characterized by the LO of *Guembelitrioides nuttalli* (Hamilton) and LO of *Acarinina bullbrooki* (Bolli), is 4 m thick (bed Pl 52 to bed Pl 58). It is equivalent to the upper part of P12 (*M. lehneri* PRZ) of Berggren *et al*. (1995) and E11 (*M. lehneri* PRZ) of Berggren & Pearson (2005) and Wade *et al*. (2011). The associated planktonic fauna contains *Globigerinatheka kugleri* (Bolli, Loeblich & Tappan), *Acarinina topilensis* (Cushman), *Turborotalia frontosa* (Subbotina), *Dentoglobigerina yeguaensis* (Weinzierl & Applin), *Acarinina bullbrooki* (Bolli), *Globigerinatheka senni* (Beckmann) and *Hantkenina* sp. This association extends through the Late Lutetian–Bartonian age.

Remarks. Zone E12 (*Orbulinoides beckmanni* Taxon-range Zone) of Berggren & Pearson (2005) and Wade *et al*. (2011) was not found in our specimens due to lateral facies change of pelagic carbonates of the Pabdeh Formation to benthic foraminiferal facies of Jahrum Formation. This zone is replaced by an inter-fingered lens of the Jahrum Formation. This interval has a thickness of 2.5 m (bed Pl 59 to bed Pl 60). The benthic foraminifera consist of *Gyrodinella magna* (Le Calvez), *Neorotalia* spp., *Asterigerina rotula* (Kaufmann), and *Discocyclina* sp. and are assigned to the Bartonian.

Pp12: *Morozovella crassata–Globigerinatheka kugleri* (IZ)

Estimated age. 40.0–38.0 Ma (Cande & Kent, 1995); 39.4–37.7 Ma (Luterbacher *et al*., 2004); 40.0–38.1 Ma (Pälike *et al*., 2006); Middle Eocene (Bartonian) (Wade *et al*., 2011).

This zone is marked by the FO of *Morozovella crassata* (Cushman) and the LO of *Globigerinatheka kugleri* (Bolli, Loeblich & Tappan), and has a thickness of 14 m (bed Pl 61 to bed Pl 76). This zone is equivalent to P14 (*Tr. rohri–M. spinulosa* PRZ) of Berggren *et al*. (1995), Zone E13 (*M. crassata* HOZ) of Berggren & Pearson (2005) and Zone E13 (*Morozovelloides crassatus* HOZ) of Wade *et al*. (2011). The biostratigraphic range is assigned to the Bartonian.

The planktonic fauna is as follows: *Globigerinatheka kugleri* (Bolli, Loeblich & Tappan), *Morozovella crassata* (Cushman), *Catapsydrax dissimilis* Cushman & Bermudez, *Dentoglobigerina yeguaensis* (Weinzierl & Applin), *Subbotina eocaenica* (Guembel), *Turborotalia pomeroli* Toumarkine & Bolli, *Turborotalia griffinae* Blow, *Pseudohastigerina micra* (Cole), *Turborotalia increbescens* Bandy, *Globigerinatheka index* (Finlay), *Globigerinatheka mexicana* (Cushman), *Globigerinatheka luterbacheri* Bolli, *Turborotalia cerroazulensis* (Cole), *Pseudohastigerina* sp. and *Hantkenina* sp.

In this interval (from bed Pl 61 to bed Pl 76), two inter-fingered lenses of Jahrum Formation containing benthic foraminifera are observed. The first lens contains *Gyrodinella magna* (Le Calvez), *Asterigerina rotula* (Kaufmann), *Gypsina marianensis* Hanzawa, *Nummulites fossulata* De Cizancourt, and *Discocyclina* sp. It has a thickness of 3.5 m and extends from bed Pl 64 to bed 68. The second level contains *Neorotalia* spp., *Discocyclina* sp., *Gyroidinella magna* (Le Calvez), *Gypsina marianensis* Hanzawa, and *Asterocyclina sireli* Özcan & Less. It presents a thickness of 3.5 m and extends from bed Pl 72 to Pl 74. Based on benthic foraminiferal association, the biostratigraphic range of both lenses is considered Bartonian.

Pp13: *Cribrohantkenina inflata–Globigerinatheka mexicana* Zone (IZ)

Estimated age. 38.0–35.8 Ma (Cande & Kent, 1995); 37.7–35.8 Ma (Luterbacher *et al*., 2004); 38.1–35.8 Ma (Pälike *et al*., 2006); Middle-Late Eocene (Bartonian–Priabonian) (Wade *et al*., 2011).

This zone, characterized by FO of *Cribrohantkenina inflata* (Howe) to LO of *Globigerinatheka mexicana* (Cushman) is 4.5 m thick (bed Pl 75 to bed Pl 83). It is equivalent to Zone P15 (*Po. semiinvoluta* IZ) of Berggren *et al*. (1995) and Zone E14 (*G. semiinvoluta* HOZ) of Berggren & Pearson (2005) and Wade *et al*. (2011). The associated planktonic fauna contains *Turborotalia cerroazulensis* (Cole), *Turborotalia pomeroli* (Toumarkine & Bolli), *Catapsydrax dissimilis* Cushman & Bermudez, *Globigerinatheka index* (Finlay), *Turborotalia increbescens* Bandy, *Globigerina* (*Dentoglobigerina*) *venezuelana* (Hedberg), and *Cribrohantkenina inflata* (Howe). This association extends through the late Bartonian–Priabonian.

Pp14: *Globigerinatheka index* Zone (PRZ)
PRZ: Partial Range Zone

This zone is characterized by the partial range of the nominate taxa between the LO of *Globigerinatheka mexicana* (Cushman) and the LO of *Globigerinatheka luterbacheri* Bolli, and it extends over a thickness of 10 m (bed Pl 83 to bed Pl 99). The associated planktonic fauna is *Pseudohastigerina naguewichiensis* (Myatliuk), *Cribrohantkenina inflate* (Howe), *Turborotalia cocoaensis* (Cushman), *Turborotalia cerroazulensis* (Cole), *Globigerina* (*Dentoglobigerina*) *venezuelana* (Hedberg), *Pseudohastigerina micra* (Cole), *Turborotalia pomeroli* (Toumarkine & Bolli), *Catapsydrax dissimilis* Cushman & Bermudez, *Turborotalia increbescens* Bandy, *Globigerinatheka mexicana* (Cushman) and *Globigerinatheka luterbacheri* Bolli.

Two levels with benthic foraminifera are observed in this biozone. The first level is 4.5 m thick and extends from bed Pl 85 to bed 90. It consists of *Fabiania cubensis* (Cushman & Bermudez), *Chapmanina gassinensis* (Silvestri), *Penarchaias* cf. *glynnjonesi* (Henson), *Praebullalveolina afyonica* Sirel & Acar, *Halkyardia* sp., *Silvestriella* cf. *tetraedra* Gumbel, *Discocyclina nandori* Less, *Nummulite*s cf. *fabianii* (Prever), *Borelis* sp., *Gyroidinella magna* (Le Calvez), *Neortalia* spp., *Praerhapydionina* sp., and *Discocyclina* sp. The second level presents a thickness of 1.5 m and extends from bed 94 to bed 97. It contains *Chapmanina gassinensis* (Silvestri), *Nummulite*s cf. *fabianii* (Prever), and *Neorotalia* spp. The aforementioned association is equivalent to E15 of Berggren & Pearson (2005) and Wade *et al*. (2011) and can be assigned to the Priabonian due to the presence of *Nummulite*s cf. *fabianii* (Prever).

The rest of the columnar section (top of section), with a thickness of 22.5 m (bed 100 to bed 111), is formed by the Jahrum Formation. It contains *Alveolina nuttalli* (Davies), *Discocyclina* cf. *nandori* Less, *Asterigerina rotula* (Kaufmann), *Macetadiscus* cf. *incolumnatus* Hottinger, *Asterocyclina sireli* Özcan & Less, and *Discocyclina* sp. The range of this association is assigned to the Priabonian based on its stratigraphic position that is on the level containing *Nummulite*s cf. *fabianii* (Prever) and the presence of *Discocyclina* cf. *nandori* Less (Özcan *et al*., 2007). The micrographs of thin sections of Paleogene planktonic and benthic foraminiferal species are shown in Figures 7–10.

DISCUSSION

Lithologic units may change laterally progressively or abruptly (Boggs, 2006). They display lateral change features such as: lateral gradation, pinch-out, and inter-tonguing/inter-fingering. The abrupt contacts (inter-tonguing) can distinctly separate two formations with different lithologies. They formed as a result of changes in local depositional conditions. Thus, the abrupt contacts are commonly very sharp.

The section studied covers mainly the Pabdeh Formation with some inter-fingered tongues of the Jahrum Formation. Based on lithological features, the Pabdeh Formation is subdivided into two lithological units (Lower and Upper Units) (Figure 2). The Lower Unit is dominated by argillaceous limestone and radiolarian chert, whereas the Upper Unit consists of argillaceous limestone, mudstone, and some inter-fingered lenses of bioclastic limestone, which are attributed to the Jahrum Formation. Therefore, the stratigraphical analysis of the Pabdeh Formation showed some inter-fingering of the benthic foraminifera bearing Jahrum Formation, which relate to the neritic deposits of the shallow marine environment. The occurrence of inter-fingered tongues of the neritic Jahrum Formation within pelagic Pabdeh

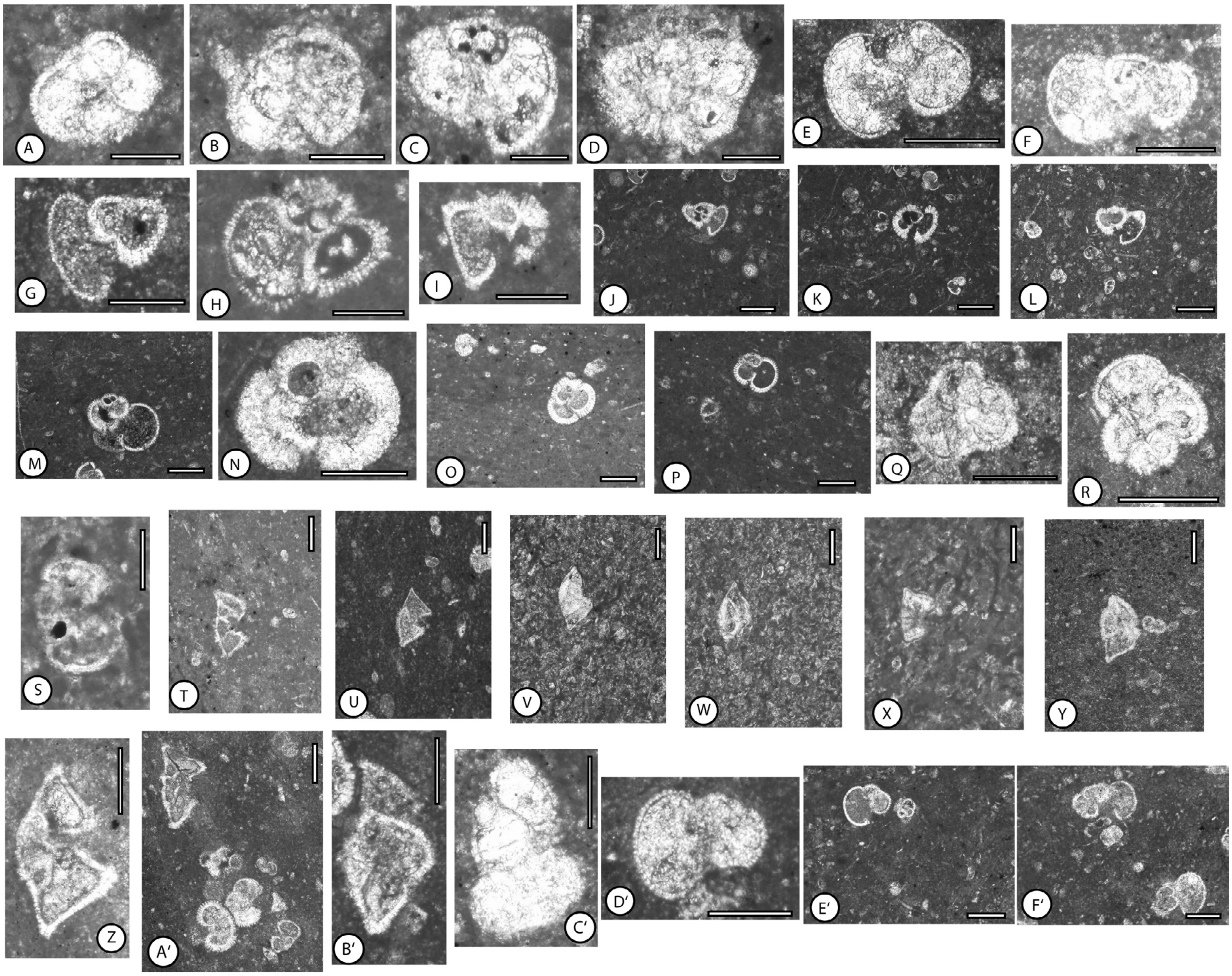

Figure 7. Microscopic images of selected planktonic foraminiferal species. **A**, *Acarinina subsphaerica* (Subbotina), Pl 3, Late Paleocene–Early Eocene; **B**, *Acarinina* cf. *nitida* (Martin), Pl 3, Late Paleocene–Early Eocene; **C**, *Acarinina mckannai* (White), Pl 2, Late Paleocene–Early Eocene; **D**, *Acarinina decepta* (Martin), Pl 2, Late Paleocene–Middle Eocene (Lutetian); **E**, *Acarinina pentacamerata* (Subbotina), Pl 20, Early Eocene; **F**, *Acarinina collactea* (Finaly), Pl 20, Early Eocene–Oligocene; **G**, *Acarinina bullbrooki* (Bolli), Pl 23, Early Eocene–Middle Eocene (Lutetian-early Bartonian); **H**, *Acarinina bullbrooki* (Bolli), Pl 28, Early Eocene–Middle Eocene (Lutetian-early Bartonian); **I**, *Acarinina pseudotopilensis* Subbotina, Pl 26, Early Eocene (Late Ypresian); **J**, *Acarinina topilensis* (Cushman), Pl 51, Middle Eocene (Lutetian); **K**, *Acarinina topilensis* (Cushman), Pl 46, Middle Eocene (Lutetian); **L**, *Acarinina spinuloinflata* (Bandy), Pl 46, Early Eocene–Middle Eocene (Bartonian); **M**, *Dentoglobigerina yeguaensis* (Weinzierl & Applin), Pl 49, Early Eocene–Oligocene; **N**, *Globigerinatheka senni* (Beckmann), Pl 38, Early Eocene–Middle Eocene (Bartonian); **O**, *Globigerinatheka kugleri* (Bolli, Loeblich & Tappan), Pl 40, Middle Eocene (Lutetian–Bartonian); **P**, *Globigerinatheka index* (Finlay), Pl 40, Middle–Late Eocene (Lutetian–Bartonian–Priabonian); **Q**, *Guembelitrioides lozanoi* (Colom), Pl 14, Early–Middle Eocene; **R**, *Guembelitrioides nuttalli* (Hamilton), Pl 22, Middle Eocene (Lutetian); **S**, *Igorina (Pearsonites) broedermanni* (Cushman & Bermudez), Pl 10, Late Paleocene–Middle Eocene; **T**, *Morozovella marginodentata* (Subbotina), Pl 10, Late Paleocene–Early Eocene; **U**, *Morozovella formosa* (Bolli), Pl 10, Early Eocene; **V**, *Morozovella edgari* (Premoli Silva & Bolli), Pl 9, Early Eocene; **W**, *Morozovella acuta* (Toulmin), Pl 9, Late Paleocene–Early Eocene; **X**, *Morozovella velascoensis* (Cushman), Pl 6, Late Paleocene–Early Eocene; **Y**, *Morozovella subbotinae* (Morozova), Pl 14, Late Paleocene–Early Eocene; **Z**, *Morozovella aragonensis* (Nuttall), Pl 27, Early Eocene–Middle Eocene (Lutetian); **A'**, *Morozovella caucasica* (Glaessner), Pl 27, Early Eocene–Middle Eocene (Lutetian); **B'**, *Planorotalites palmerae* Cushman & Bermudez, Pl 21, late Early Eocene; **C'**, *Turborotalia prolata* (Belfoed), Pl 18, Late Paleocene–Early Eocene; **D'**, *Turborotalia frontosa* (Subbotina), Pl 23, Early Eocene–Middle Eocene (Lutetian); **E'**, *Turborotalia frontosa* (Subbotina), Pl 43, Early Eocene–Middle Eocene (Lutetian); **F'**, *Turborotalia possagnoensis* (Toumarkine & Bolli), Pl 43, Middle Eocene (Lutetian). Scale bars: A, B, E, F, G, I, N, Q, R, S, C', D' = 200 µm; H, Z = 250 µm; C, D, J, K, L, M, O, P, T, U, V, W, X, Y, A', E', F'= 160 µm; B' = 170 µm.

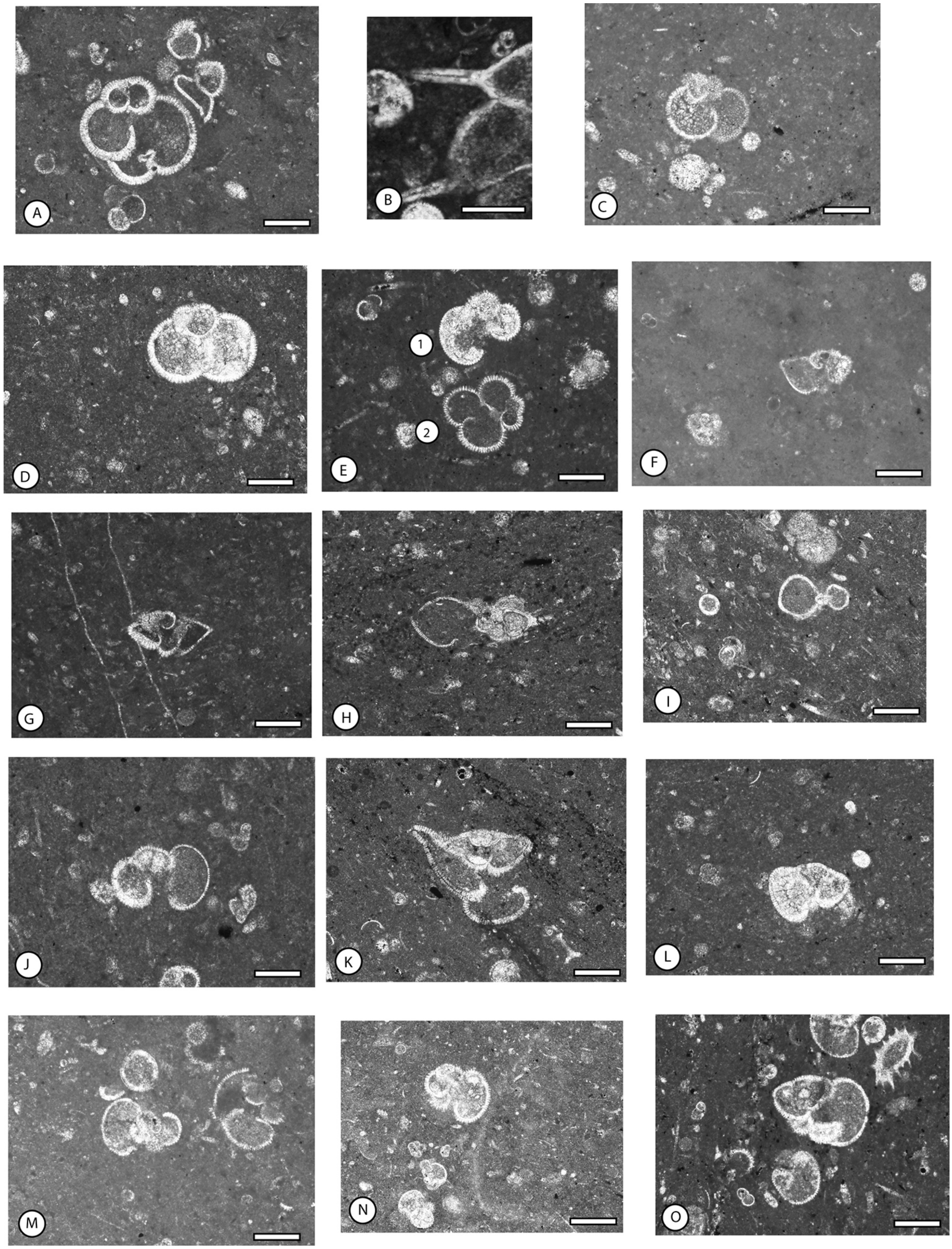

Figure 8. Microscopic images of selected planktonic foraminiferal species. **A**, *Catapsydrax dissimilis* Cushman & Bermudez, Pl 62, Middle Eocene (Bartonian)–Oligocene; **B**, *Cribrohantkenina inflata* Howe, Pl 77, Bartonian–Priabonian; **C**, *Globigerinatheka luterbacheri* Bolli, Pl 76, Lutetian–Priabonian; **D**, *Globigerina venezuelana* (Hedberg), Pl 82, Late Eocene–Oligocene; **E1**, *Globigerina praebulloides* Blow, Pl 51, Middle Eocene–Oligocene; **E2**, *Guembelitrioides nuttalli* (Hamilton), Pl 51, Middle Eocene (Lutetian); **F**, *Morozovella crassata* (Cushman), Pl 61, Early Eocene–Middle Eocene (Bartonian); **G**, *Morozovella* (*Morozovelloides*) *lehneri* (Cushman & Jarvis), Pl 49, Middle Eocene (Lutetian–Bartonian); **H**, *Pseudohastigerina naguewichiensis* (Myatliuk), Pl 83, Priabonian–Oligocene; **I**, *Pseudohastigerina micra* (Cole), Pl 70, Early Eocene–Oligocene; **J**, *Subbotina eocaenica* (Guembel), Pl 63, Early Eocene–Oligocene; **K**, *Turborotalia cocoaensis* (Cushman), Pl 83, Bartonian–Priabonian; **L**, *Turborotalia cerroazulensis* (Cole), Pl 76, Lutetian–Priabonian; **M**, *Turborotalia griffinae* Blow, Pl 69, Middle Eocene; **N**, *Turborotalia increbescens* Bandy, Pl 70, Middle Eocene (Bartonian)–Oligocene; **O**, *Turborotalia pomeroli* Toumarkine & Bolli, Pl 70, Middle Eocene–Late Eocene. Scale bars: A–I; K–O = 160 µm; J = 200 µm.

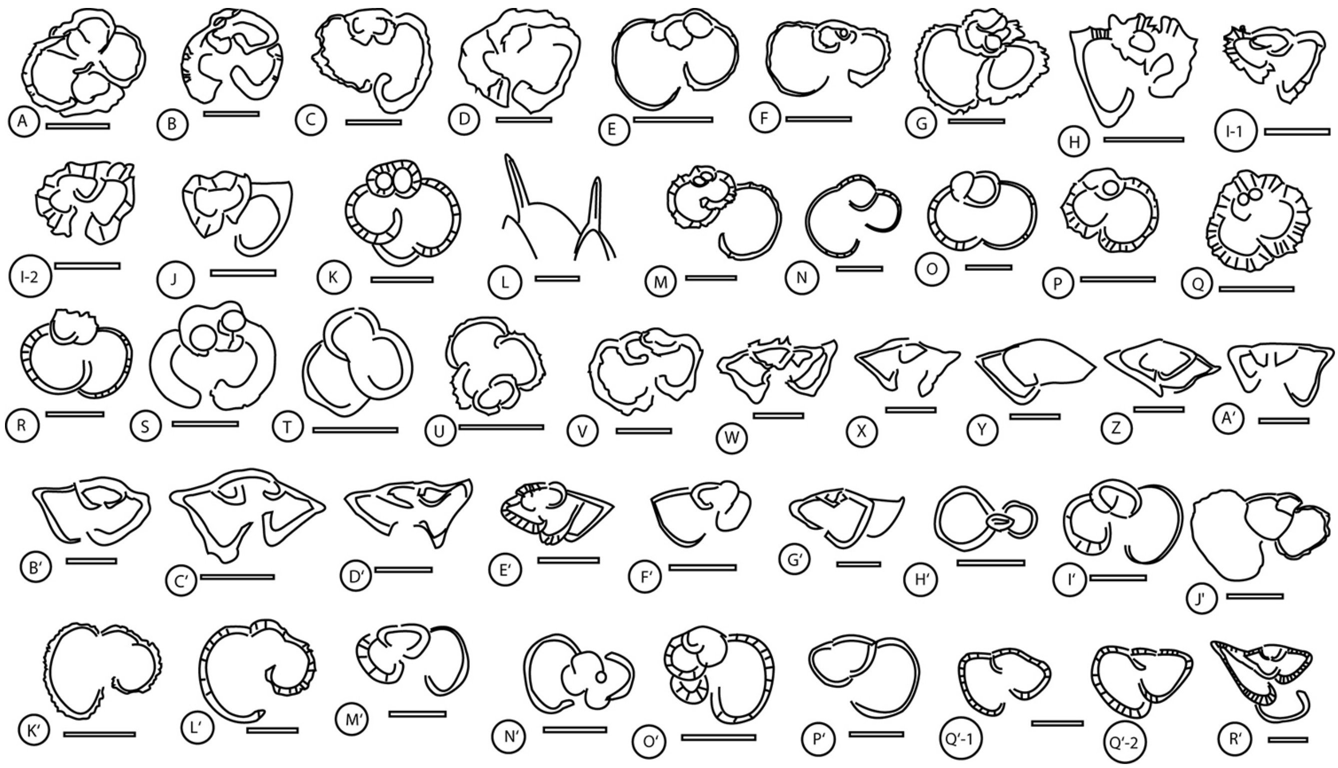

Figure 9. Drawings of thin sections of selected planktonic foraminiferal species. **A**, *Acarinina subsphaerica* (Subbotina), Pl 3, Late Paleocene–Early Eocene; **B**, *Acarinina* cf. *nitida* (Martin), Pl 3, Late Paleocene–Early Eocene; **C**, *Acarinina mckannai* (White), Pl 2, Late Paleocene–Early Eocene; **D**, *Acarinina decepta* (Martin), Pl 2, Late Paleocene–Middle Eocene (Lutetian); **E**, *Acarinina pentacamerata* (Subbotina), Pl 20, Early Eocene; **F**, *Acarinina collactea* (Finaly), Pl 20, Early Eocene–Oligocene; **G**, *Acarinina bullbrooki* (Bolli), Pl 28, Early Eocene–Middle Eocene (Bartonian); **H**, *Acarinina pseudotopilensis* Subbotina, Pl 26, Early Eocene (Late Ypresian); **I1** & **I2**, *Acarinina topilensis* (Cushman), Pl 46, Middle Eocene (Lutetian); **J**, *Acarinina spinuloinflata* (Bandy), Pl 46, Early Eocene–Middle Eocene (Bartonian); **K**, *Catapsydrax dissimilis* Cushman & Bermudez, Pl 62, Middle Eocene (Bartonian)–Oligocene; **L**, *Cribrohantkenina inflata* Howe, Pl 77, Bartonian–Priabonian; **M**, *Dentoglobigerina yeguaensis* (Weinzierl & Applin), Pl 49, Early Eocene–Oligocene; **N**, *Globigerina praebulloides* Blow, Pl 51, Middle Eocene–Oligocene, 160 mm; **O**, *Globigerina venezuelana* (Hedberg), Pl 82, Late Eocene–Oligocene; **P**, *Globigerinatheka index* (Finlay), Pl 40, Middle–Late Eocene (Lutetian–Bartonian–Priabonian); **Q**, *Globigerinatheka kugleri* (Bolli, Loeblich & Tappan), Pl 40, Middle Eocene (Lutetian-Bartonian); **R**, *Globigerinatheka luterbacheri* Bolli, Pl 76, Lutetian–Priabonian; **S**, *Globigerinatheka senni* (Beckmann), Pl 38, Early Eocene–Middle Eocene (Bartonian); **T**, *Guembelitrioides lozanoi* (Colom), Pl 14, Early–Middle Eocene; **U**, *Guembelitrioides nuttalli* (Hamilton), Pl 22, Middle Eocene (Lutetian); **V**, *Igorina (Pearsonites) broedermanni* (Cushman & Bermudez), Pl 10, Late Paleocene–Middle Eocene; **W**, *Morozovella marginodentata* (Subbotina), Pl 10, Late Paleocene–Early Eocene; **X**, *Morozovella formosa* (Bolli), Pl 10, Early Eocene; **Y**, *Morozovella edgari* (Premoli Silva & Bolli), Pl 9, Early Eocene; **Z**, *Morozovella acuta* (Toulmin), Pl 9, Late Paleocene–Early Eocene; **A'**, *Morozovella velascoensis* (Cushman), Pl 6, Late Paleocene–Early Eocene; **B'**, *Morozovella subbotinae* (Morozova), Pl 14, Late Paleocene–Early Eocene; **C'**, *Morozovella aragonensis* (Nuttall), Pl 27, Early Eocene–Middle Eocene (Lutetian); **D'**: *Morozovella caucasica* (Glaessner), Pl 27, Early Eocene–Middle Eocene (Lutetian); **E'**, *Morozovella* (*Morozovelloides*) *lehneri* (Cushman & Jarvis), Pl 49, Middle Eocene (Lutetian–Bartonian); **F'**, *Morozovella crassata* (Cushman), Pl 61, Early Eocene–Middle Eocene (Bartonian); **G'**, *Planorotalites palmerae* Cushman & Bermudez, Pl 21, late Early Eocene; **H'**, *Pseudohastigerina micra* (Cole), Pl 70, Early Eocene–Oligocene; **I'**, *Subbotina eocaenica* (Guembel), Pl 63, Early Eocene–Oligocene; **J'**, *Turborotalia prolata* (Belfoed), Pl 18, Late Paleocene–Early Eocene; **K'**, *Turoborotalia frontosa* (Subbotina), Pl 23, Early Eocene–Middle Eocene (Lutetian); **L'**: *Turoborotalia frontosa* (Subbotina), Pl 43, Early Eocene–Middle Eocene (Lutetian); **M'**, *Turborotalia possagnoensis* (Toumarkine & Bolli), Pl 43, Middle Eocene (Lutetian); **N'**, *Turborotalia griffinae* Blow, Pl 69, Middle Eocene; **O'**, *Turborotalia increbescens* Bandy, Pl 70, Middle Eocene (Bartonian)–Oligocene; **P'**, *Turborotalia pomeroli* Toumarkine & Bolli, Pl 70, Middle Eocene–Late Eocene; **Q'1** & **Q'2**, *Turborotalia cerroazulensis* (Cole), Pl 76, Lutetian–Priabonian; **R'**, *Turborotalia cocoaensis* (Cushman), Pl 83, Bartonian–Priabonian. Scale bars: A, B, E, F, H, S, T, U, V, J', K' = 200 µm; C', = 250 µm; C, D, I, J–R, W, X, Y, Z, A', D', E', F', H', I', L'–R' = 160 µm; B' = 80 µm; G = 170 µm.

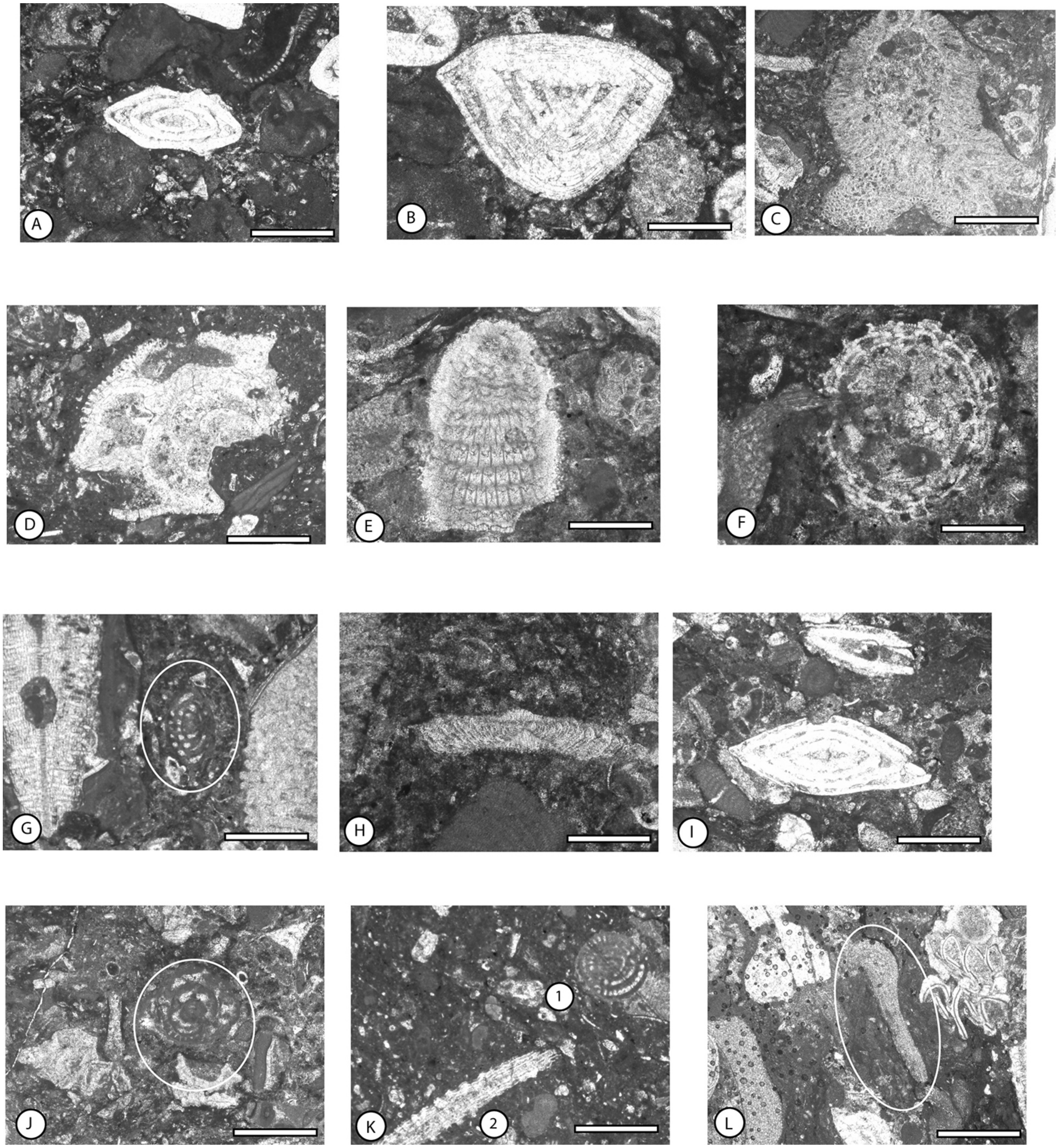

Figure 10. Microscopic images of selected benthic foraminiferal species. **A**, *Nummulites fossulata* De Cizancourt, Pl 63, Early Eocene–Middle Eocene; **B**, *Asterigerina rotula* (Kaufmann), Pl 66, Middle Eocene–Late Eocene; **C**, *Fabiania cubensis* (Cushman & Bermudez), Pl 89, Middle Eocene (Lutetian–Bartonian); **D**, *Gyrodinella magna* (Le Calvez), Pl 88, Middle Eocene–Late Eocene; **E**, *Chapmanina gassinensis* (Silvestri), Pl 89, Bartonian–Priabonian; **F**, *Silvestriella* cf. *tetraedra* Gumbel, Pl 89, Bartonian–Priabonian; **G**, *Penarchaias* cf. *glynnjonesi* (Henson), Pl 89, Middle Eocene–Oligocene; **H**, *Halkyardia* sp., Pl 89, Priabonian–Oligocene; **I**, *Nummulite*s cf. *fabianii* (Prever), Pl 95, Priabonian; **J**, *Praebullalveolina* cf. *afyonica* Sirel & Acar, Pl 89, Priabonian; **K1**, *Borelis* sp., Pl 88, Bartonian–Priabonian; **K2**, *Discocyclina* cf. *nandori* Less, Pl 88, Bartonian–Priabonian; **L**, *Gypsina marianensis* Hanzawa, Pl 66, Middle Eocene (Lutetian–Bartonian). Scale bars = 1.25 mm.

Formation suggests repeated fast depth changes. It may be postulated that lateral and vertical facies changes were due to tectonic events within the Zagros Foreland Basin. Specifically, interfingering of benthic facies within deeper basin sediments may be related to moderate tectonic subsidence while mid- to late Eocene shallowing was possibly related to the general shrinking of the basin.

The argillaceous limestones mostly contain planktonic foraminifera such as *Acarinia*, *Morozovella*, *Globigerinatheka*, *Turborotalia*, among others. The pelagic and hemipelagic facies of the Pabdeh Formation are deposited in the deep-sea environment of the open ocean.

Further up, toward the top of the section, the Pabdeh formation is overlain by the Jahrum Formation represented by a carbonate succession of medium to coarse grain bioclastic limestone (packstone facies) with large hyaline/porcellaneous foraminifers and abundant red algae.

The overlapping bioclastic limestone of Jahrum Formation on top of the section indicates a shallowing upward trend. Hence it could be due to the progressive shrinking of the basin or alternatively to sea-level drop. On the other hand, the gradual decline of micrite observed in the Jahrum Formation is likely due to decreasing water depth and increasing energy, which led to the development of bioclastic limestone. Concomitantly, the benthic foraminifers are mainly limited to hyaline foraminifers such as rotaliids (*Gyroidinella*), orthophragminid (*Discocyclina*, *Asterocyclina*), nummulitids (*Nummulites*) and porcellaneous foraminifers such as alveolinids (*Alveolina* and *Macetadiscus*), which indicate restricted platform conditions (Murray, 1991; Hottinger, 1983, 1997; Flügel, 1982, 2004). The benthic foraminifers are classified into three faunal associations based on stratigraphic position.

The benthic foraminiferal association I occurs in three intervals: bed Pl 59 to bed Pl 60, bed Pl 64 to bed 68, and bed Pl 72 to Pl 74 (Figure 3). It is characterized by the presence of *Gyrodinella magna* (Le Calvez), *Asterigerina rotula* (Kaufmann), *Nummulites fossulata* De Cizancourt, *Gypsina marianensis* Hanzawa, *Asterocyclina sireli* Özcan & Less, *Neorotalia* spp., and *Discocyclina* sp. It can be correlated with planktonic biozones E12 and E13 of Berggren & Pearson (2005) and Wade *et al*. (2011) and is assigned to the Bartonian age.

The benthic foraminiferal association II occurs in two intervals: bed Pl 85 to bed 90 and bed 94 to bed 97 (Figure 3). It is defined by the presence of *Fabiania cubensis* (Cushman & Bermudez), *Chapmanina gassinensis* (Silvestri), *Penarchaias* cf. *glynnjonesi* (Henson), *Praebullalveolina* cf. *afyonica* Sirel & Acar, *Halkyardia* sp., *Silvestriella* cf. *tetraedra* Gumbel, *Discocyclina nandori* Less, *Nummulites* cf. *fabianii* (Prever), *Borelis* sp., *Gyrodinella magna* (Le Calvez), *Neortalia* spp., *Praerhapydionina* sp., and *Discocyclina* sp. This association is equivalent to E15 of Berggren & Pearson (2005) and Wade *et al*. (2011) and assigned to the Priabonian age. The presence of *Nummulites* cf. *fabianii* (Prever) can confirm the Priabonian age.

The benthic foraminiferal association III occurs in one interval at the top of the section (Figure 3). It is characterized by the presence of *Alveolina nuttalli*, *Discocyclina* cf. *nandori* Less, *Asterigerina rotula* (Kaufmann), *Macetadiscus* cf. *incolumnatus* Hottinger, and *Discocyclina* sp. It has a thickness of 22.5 m and extends from bed 100 to bed 111. This association is equivalent to E16 of Berggren & Pearson (2005) and Wade *et al*. (2011). Based on the stratigraphic position and the presence of *Discocyclina* cf. *nandori* Less, the range of this association is assigned to the Priabonian age.

The large hyaline foraminifers such as *Discocyclina*, *Asterocyclina*, and *Nummulites*, were spread throughout the Tethyan region from the eastern Alps to the Middle East (eastern and western Iran) and occurred in a broad range of open marine environments during the Eocene (Romero *et al*., 2002; Bassi *et al*., 2007; Nebelsick *et al*., 2005). The small hyaline foraminifers such as rotaliids (*Gyroidinella* and *Asterigerina*) are not limited to a specific environment and are distributed from shallow water to an open marine environment. In contrast, the large-thin shell hyaline foraminifers (*Discocyclina* and *Asterocyclina*) are adapted to relatively deeper water than the small hyaline foraminifers, and preferred low energy environment during the Eocene (Buxton & Pedley, 1989). In the study area, *Discocyclina* and *Asterocyclina* are mainly associated with rotaliids (*Gyroidinella* and *Asterigerina*), while alveolinids and nummulitids are locally relatively common in the bioclastic facies of Jahrum Formation. The low frequency of *Nummulites* and major changes in the composition of benthic foraminifera, with an increasing amount of rotaliids, recorded a change in the sedimentary environment.

The presence of porcellaneous foraminifers indicates the meso- to oligotrophic shallow water environments (Reiss & Hottinger, 1984; Hallock, 1984, 1988; Buxton & Pedley, 1989; Romero *et al*., 2002). *Alveolina* and *Macetadiscus*, as the representative of porcellaneous foraminifers, are important taxa in Lower Paleogene shallow-water deposits. They occurred in protected shelf (lagoonal setting), enclosure behind the back shoal, and shoal environments (Hottinger, 1983).

The presence of marker planktonic foraminifera such as *Acarinina subsphaerica* (Subbotina) confirms the Late Paleocene age of Zone Pp1, because the last occurrence of this species falls in the upper part of Zone Pp1. The species *Morozovella velascoensis* (Cushman) occurs across the Late Paleocene–Early Eocene boundary, therefore its presence helps to distinguish the Zone Pp2. During the Early Eocene from the upper part of Zone Pp2 to Zone Pp7, some taxa such as *Morozovella* and *Turborotalia* were rare, but *Igorina broedermanni* (Cushman & Bermudez) was only sporadic during the Early Eocene (Ypresian).

The Lutetian stage (from Zone Pp8 to Zone Pp10) coincides with the extinction of some species such as *Planorotalites palmerae* Cushman & Bermudez, *Acarinina pseudotopilensis* Subbotina, *Turborotalia prolata* (Belfoed), and *Acarinina pentacamerata* (Subbotina). In contrast, the association of *Acarinina bullbrooki* (Bolli), *Globigerinatheka kugleri*

(Bolli, Loeblich & Tappan), *Turborotalia possagnoensis* (Toumarkine & Bolli), *Acarinina topilensis* (Cushman), *Dentoglobigerina yeguaensis* (Weinzierl & Applin), *Globigerinatheka senni* (Beckmann), *Guembelitrioides nuttalli* (Hamilton), *Turborotalia frontosa* (Subbotina), *Turborotalia possagnoensis* (Toumarkine & Bolli), and *Morozovella aragonensis* (Nuttall) are abundant.

The time interval Lutetian–Bartonian is equivalent to Zone Pp11, which is consistent with Zone E11 of Berggren & Pearson (2005). It is characterized by the partial range zone of *Morozovella lehneri* (Cushman & Jarvis).

Abundant Bartonian planktonic foraminifers are represented in the Zone Pp12 of this study, but some species such as *Turborotalia griffinae* Blow, *Pseudohastigerina micra* (Cole), *Globigerinatheka mexicana* (Cushman), *Globigerinatheka luterbacheri* Bolli, *Turborotalia increbescens* Bandy, *Turborotalia cerroazulensis* (Cole), *Pseudohastigerina* sp. and *Hantkenina* sp. are rare in this biozone. In contrast, they are abundant in the Zone Pp13 for the Bartonian–Priabonian time interval. The species *Globigerinatheka kugleri* (Bolli, Loeblich & Tappan) becomes extinct in this biozone, whereas the species *Globigerina* (*Dentoglobigerina*) *venezuelana* (Hedberg), and *Cribrohantkenina inflata* (Howe) are reported for the first time.

CONCLUSIONS

The Pabdeh Formation is mainly composed of hemipelagic and pelagic sediments with intercalations of radiolarian chert, whereas the Jahrum Formation consists of neritic deposits accumulated on a shallow marine platform. Both formations are disconformably covered by the Late Oligocene-Miocene Asmari Formation.

The Pabdeh Formation, recovered in the northwest of Shahrekord City, contains Late-Paleocene to Late Eocene planktonic foraminifera (Zone Pp1–Pp14), which correlate mainly with the subtropical to tropical Zones P4b-E15 of Berggren & Pearson (2005).

The upper part of the stratigraphic succession of the Pabdeh Formation consists of some inter-fingered lenses of the benthic foraminifera-bearing limestone of the Jahrum Formation. The lateral interfingering of Pabdeh and Jahrum formations and upward shallowing marked by the disappearance of planktonic foraminifera during the Eocene are uncorrelated to sea level variations and may be ascribed to moderate tectonic subsidence and progressive shrinking of the Zagros foreland Basin respectively. Lateral changes and bulk shallowing suggest transgression during the late Paleocene, back and forth variations during the mid-Eocene and then global regression during the late Eocene, since these variations are uncorrelated to climate-driven sea level variations (Cramwinckel *et al*., 2018).

The stratigraphic range of three benthic foraminiferal associations is assigned to Bartonian–Priabonian (Middle to Late Eocene) and can be equivalent with Zone Pp12–Zone Pp14.

Late Paleocene planktonic foraminifera are sparse in the Pabdeh Formation, whereas the Eocene planktonic foraminifers are more abundant and widespread.

During the Early Eocene, the two genera *Acarinina* and *Morozovella* are abundant, while other genera such as *Globigerinatheca* and *Turborotalia* gradually become predominant.

The absence of open marine planktonic foraminifera such as *Orbulinoides beckmanni*, that characterizes the Zone E12 of Berggren & Pearson (2005) in the upper unit of the Pabdeh Formation, coincides with the sudden appearance of larger benthic foraminifera coeval with coarsening upwards trend.

ACKNOWLEDGEMENTS

We thank B.A. Pirbaloti, M. Soltani, and Z. Shaiesteh Nia for their generous help during fieldwork. We thank two anonymous referees who enabled us to improve the manuscript. The first author is grateful for the facilities provided by the Department of Geology of Payame Noor University. This research did not receive any specific grant from funding agencies in the public, commercial, or non-profit sectors.

REFERENCES

Adams, T.D. & Bourgeois, F. 1967. Asmari biostratigraphy, geological and exploration division. *Iranian Oil Offshore Company Report*, **1074** (Unpublished).

Ahmad, S.; Jalal, W.; Ali, F.; Hanif, M.; Ullah, Z.; Khan, S.; Ali, A.; Jan, UI. & Rehman, K. 2014. Using larger benthic foraminifera for the paleogeographic reconstruction of Neo-Tethys during Paleogene. *Arabian Journal Geoscience*, **8**:5095–5110. *doi:10.1007/s12517-014-1549-x*

Alavi, M. 2004. Regional stratigraphy of Zagros Fold-Thrust Belt of Iran and its proforel and evolution. *American Journal of Science*, **304**:1–20. *doi:10.2475/ajs.304.1.1*

Babazadeh, S.A. 2003. *Biostratigraphie et contrôles paléogéographiques de la zone de suture de l'Iran oriental. Implications sur la fermeture Téthysienne*. Université d'Orléans, Ph.D. Thesis, 384 p.

Babazadeh, S.A.; Baharan, S.; Parvaneh Nezhad Shirazi, M. & Bahrami, M. 2010. Biostratigraphy of Pabdeh Formation in Tange Zanjiran section (southeast Shiraz) based on planktic foraminifera. *Sedimentology and Stratigraphy Research*, **38**:145–158.

Babazadeh, S.A.; Moghadasi, S.J. & Yoosefizadeh Baghestani, N. 2015. Analysis of sedimentary basin based on the distribution of microfacies of Jahrom Formation in Dashte Zari, Shahrekord. *In*: GEOLOGY CONFERENCE OF IRAN, 18, 2015. *Abstracts*, Tarbiat Modares University, p. 649–655.

Bassi, B.; Braga, J.C.; Zakrevskaya, E. & Radionova, E.P. 2007. Redescription of the type collections of Maslov's species of Corallinales (Rhodophyta). II. Species included by Maslov in *Archaeolithothamnium* Rothpletz, 1891. *Revista Espanola de Paleontologia*, **22**:115–125. *doi:10.7203/sjp.22.2.20417*

Berberian, M. 1995. Master "blind" thrust faults hidden under the Zagros folds: active basement tectonics and surface morphotectonics. *Tectonophysics*, **241**:193–224. *doi:10.1016/0040-1951(94)00185-C*

Berberian, M. & King, G.C.P. 1981. Towards a paleogeography and tectonic evolution of Iran. *Canadian Journal of Earth Sciences*, **18**:210–265. *doi:10.1139/e81-019*

Berggren, W.A.; Kent, D.V.; Swisher, I.C.C. & Aubry, M.P. 1995. A revised Cenozoic geochronology and chronostratigraphy. *In*: W.A. Berggren; D.V. Kent; M.P. Aubry & J. Hardenbol (eds.) *Geochronology Time Scales and Global Stratigraphic Correlations*, Society of Economic Paleontologists and Mineralogists Special Publication, vol. 54, p. 129–212.

Berggren, W.A. & Pearson, P. 2005. A revised tropical to subtropical paleogene planktonic foraminiferal zonation. *The Journal of Foraminiferal Research*, **35**:279–298. *doi:10.2113/35.4.279*

Berggren, W.A.; Pearson, P.N.; Huber, B.T. & Wade, B.S. 2006. Taxonomy, biostratigraphy, and phylogeny of Eocene *Acarinina*. *Cushman Foundation Special Publication*, **41**:257–326.

Boggs, S. 2006. *Principles of Sedimentology and Stratigraphy.* 3 ed. Pearson Education, 676 p.

Buxton, M.W.N. & Pedley, H.M. 1989. Short paper: a standardised model for Tethyan Tertiary carbonate ramps. *Journal of the Geological Society of London*, **146**:746–748.

Cande, S.C. & Kent, D.V. 1995. Revised calibration of the geomagnetic polarity timescale for the Late Cretaceous and Cenozoic. *Journal of Geophysical Research*, **100**:6093–6095. *doi:10.1029/94JB03098*

Chegni, F.; Baghbani, D.; Vaziri, S.H.; Mohtat, T. & Ghadimvand Kohansal, N. 2016. Biostratigraphy of Pabdeh Fm. (Middle-Late Eocene) in south Kuh-e-Mishan and Kuh-e-Eshgar in Izeh, west Kazeron fault. *Earth sciences, Geological Survey of Iran*, **99**:143–156.

Cole, W.S. & Gravell, D.W. 1952. Middle Eocene Foraminifera from Peñon Seep, Matanzas Province, Cuba. *Journal of Paleontology,* **26**:708–727.

Cramwinckel, M.J. *et al*. 2018. Synchronous tropical and polar temperature evolution in the Eocene. *Nature*, **559**:382–386. *doi:10.1038/s41586-018-0272-2*

Daneshian, J.; Shariati, S. & Salsani, A. 2015. Biostratigraphy and planktonic foraminiferal abundance in the phosphate-bearing Pabdeh Formation of the Lar Mountains (SW Iran). *Neues Jahrbuch für Geologie und Paläontologie, Abhandlungen*, **278**:1–16. *doi:10.1127/njgpa/2015/0522*

Davoudzadeh, M. & Schmidt, K. 1981. Contribution to the paleogeography andstratigraphy of the Upper Triassic to Middle Jurassic of Iran. *Neues Jahrbuch fur Geologie und Palaontologie, Abhandlungen*, **162**:137–163.

Ehrennberg, S.N.; Pickard, N.A.H.; Laursen, G.V.; Monibi, S.; Mossadegh, Z.K.T.; Svånå, A.; Aqrawi, A.A.M.; McArthur, J.M. & Thirlwall, M.F. 2007. Strontium isotope stratigraphy of the Asmari Formation (Oligocene - Lower Miocene), SW Iran. *Journal of Petroleum Geology*, **30**:107–128. *doi:10.1111/j.1747-5457.2007.00107.x*

Ellis, B.F. & Messina, A. 1940. *Catalogue of Foraminifera*. New York, Micropaleontology Press, American Museum of Natural History.

Flügel, E. 1982. *Microfacies analysis of limestones*. Berlin, Springer-Verlag, 633 p.

Flügel, E. 2004. *Microfacies of carbonate rock*. Berlin, Springer-Verlag, 976 p.

Hadavandkhani, N.; Sadeghi, A.; Adabi, M.H. & Tahmasbi, A.R. 2018. Lithostratigraphy and biostratigraphy of Pabdeh Formation in Chaharda village section (Izeh, Khuzestan). *Earth sciences, Geological Survey of Iran*, **107**:137–150.

Hanzawa, S. 1957. Cenozoic Foraminifera of Micronesia. *Geological Society of America,* **66**:1–163.

Hayward, B.W.; Le Coze, F.; Vachard, D. & Gross, O. 2021. World Foraminifera Database. *Fabiania cubensis*. Available at https://marinespecies.org/foraminifera/aphia; accessed on 17/02/2021.

Hallock, P. 1984. Distribution of selected species of living algal symbiont–bearing foraminifera on two Pacific coral reefs. *Journal of Foraminiferal Research*, **9**:61–69.

Hallock, P. 1988. Diversification in algal symbiont-bearing foraminifera: a response to oligotrophy? *Revue de Paléobiologie*, **2**:789–797.

Hottinger, L. 1983. Processes determining the distribution of larger foraminifera in space and time. *Utrecht Micropaleontological Bulletin*, **30**:239–253.

Hottinger, L. 1997. Shallow benthic foraminiferal assemblages as signals for depth of their deposition and their limitations. *Bulletin de la Société Géologique de France*, **168**:491–505.

Hottinger, L. 2007. Revision of the foraminiferal genus *Globoreticulina* Rahaghi, 1978, and of its associated fauna of larger foraminifera from the late Middle Eocene of Iran. *Notebooks on Geology*, **7**:A06.

James, G.A. & Wynd, J.G. 1965. Stratigraphic Nomenclature of Iranian Oil Consortium Agreement Area. *American Association of Petroleum Geologists Bulletin*, **49**:94–156.

Kalantari, A. 1975. Microbiostratigraphy of the Sarvestan Area, Southwestern Iran. *Geological Laboratories Publication, National Iranian Oil Company*, **5**:1–129.

Kalantari, A. 1986. Microfacies of Carbonate Rocks of Iran. *Geological Laboratories Publication, National Iranian Oil Company*, 1–520.

Khatibi Mehr, M. & Moalemi, A. 2009. Historical sedimentary correlation between Jahrom Formation and Ziarat Formation on the basis of benthic foraminifera. *Journal of Geology of Iran*, **9**:87–102.

Konijnenburg, J.H.V.; Wernli, R. & Bernoulli, D. 1998. Tentative biostratigraphy of Paleogene planktic foraminifera in thin-section, an example from the Gran Sasso d'Italia (central Apennines, Italy). *Eclogae Geologicae Helvetiae*, **91**:203–216.

Le Calvez, Y. 1949. Révision des foraminifères lutétiens du Bassin de Paris II, Rotaliidae et familles affines. *Mémoires pour servir à l'explication de la carte géologique détaillée de la France*, 1–41.

Loeblich, A.R. & Tappan H. 1987. *Foraminiferal genera and their classification*. New York, Van Nostrand Reinhold Co., 970 p.

Luterbacher, H.P. *et al*. 2004. The Paleogene Period. *In*: F. Gradstein; J. Ogg & A. Smith (eds.) *A Geologic Time Scale*, Cambridge University Press, p. 384–408.

Moradian, F. & Baghbani, D. 2016. Lithostratigraphy, biostratigraphy of Paleocene-lower Eocene sequences in Dezful embayment, southwest Iran. *Iranian Journal of Earth Sciences*, **8**:135–146.

Moradian, F.; Baghbani, D. & Allameh, M. 2017. Microbiostratigrapy of the Paleocene-Lower Eocene sequences in the Bibi Hakimeh 2 subsurface section located in the SW of Iran. *Open Journal of Geology*, **7**:147–161. *doi:10.4236/ojg.2017.72010*

Motiei, H. 1993. *Stratigraphy of Zagros*. *Treatise of Geology of Iran*. Tehran, Geological Survey of Iran Publication, 559 p.

Murray, J.W. 1991. *Ecology and Palaeoecology of Benthic Foraminifera*. London, Longman Science & Technology, 397 p.

Nebelsick, J.H.; Rasser, M. & Bassi, D. 2005. Facies dynamics in Eocene to Oligocene Circumalpine carbonates. *Facies*, **51**:197–216.

Olsson, R.K.; Hemleben, C.; Berggren, W.A. & Huber, B.T. 1999. *Atlas of Paleocene Planktonic Foraminifera.* Washington DC, Smithsonian Institution Press, 252 p.

Ozcan, E.; Less, G.; Baldi-Beke, M.; Kollanyi, K. & Kertesz, B. 2007. Biometric analysis of middle and upper Eocene Discocyclinidae and Orbitoclypeidae (Foraminifera) from Turkey and updated orthophragmine zonation in the Western Tethys. *Micropaleontology*, **52**:485–520.

Ozgen, N. 2000. *Nurdanella boluensis* n. gen., n. sp., a Miliolid (Foraminifera) from the Lutetian of the Bolu Area (Northwestern Turkey). *Revue de Paléobiologie*, **19**:79–85.

Pälike, H.; Norris, R.D.; Herrle, J.O.; Wilson, P.A., Coxall, H.K.; Lear, C.H.; Shackleton, N.J.; Tripati, A.K. & Wade, B.S. 2006. The heartbeat of the Oligocene climate system. *Science*, **314**: 1894–1898. *doi:10.1126/science.1133822*

pforams@mikrotax. Available at https://mikrotax.org/pforams/index.php?id=100241; accessed on 17/02/2021.

Postuma, S.A. 1971. *Manual of Planktonic Foraminifera*. Amsterdam, Elsevier, 420 p.

Premoli Silva, I. & Bolli, H.M. 1973. Late Cretaceous to Eocene planktonic foraminifera and stratigraphy of leg 15, Sites in the Caribbean Sea. *Initial Reports DSDP*, **15**:449–547.

Premoli Silva, I.; Rettori, R. & Verga, D. 2003. *Practical Manual of Paleocene and Eocene Planktonic Foraminifera*. Perugia, International School on planktonic foraminifera, 2nd course.

Rahaghi, A. 1976. Contribution a l'étude de quelques grands foraminiferes de L'Iran. *National Iranian Oil Company*, **6**:1–84.

Rahaghi, A. 1978. Paleogene biostratigraphy of some parts of Iran. *National Iranian Oil Company*, **7**:1–165.

Rahaghi, A. 1980. Tertiary faunal assemblage of Qom-Kashan, Sabzewar and Jahrom area. *National Iranian Oil Company*, **8**:1–126.

Rahaghi, A. 1983. Stratigraphy and faunal assemblage of Paleocene and Lower Eocene in Iran. *National Iranian Oil Company*, **10**:1–173.

Reiss, Z. & Hottinger, L. 1984. *The Gulf of Aqaba: ecological micropaleontology*. Ecological studies, vol 50. Springer, Berlin, 354 p.

Romero, J.; Caus, E. & Rosell, J. 2002. A model for the palaeoenvironmental distribution of larger foraminifera based on late Middle Eocene deposits on the margin of the South Pyrenean basin (NE Spain). *Palaeogeography*, *Palaeoclimatology*, *Palaeoecology*, **179**:43–56. *doi:10.1016/S0031-0182(01)00406-0*

Sari, B. 2017. Lithostratigraphy and planktonic foraminifera of the uppermost Cretaceous–Upper Palaeocene strata of the Tavas nappe of the Lycian nappes (SW Turkey). *Geologia Croatica*, **70**:163–177. *doi:10.4154/gc.2017.14*

Sarigül, V.; Hakyemez, A.; Tuysuz, O.; Can Genc, S.; Yilmaz, I.O. & Ozcan, E. 2017. Maastrichtian-Thanetian planktonic foraminiferal biostratigraphy and remarks on the K-Pg boundary in the southern Kocaeli Peninsula (NW Turkey). *Turkish Journal of Earth Sciences*, **26**:1–29. *doi:10.3906/yer-1602-23*

Sengor, A.M.; Altiner, C; Cin, D.; Ustomer, T. & Hsu, K.J. 1988. The origin and assembly of the Tethyside orogenic collage at the expense of Gondwana land. *In*: M.G. Audley-Charles & A. Hallam (eds.) *Gondwana and Tethys*, Geological Society, Special Publication, vol. 37, p. 119–181.

Serra-Kiel, J.S.; Cañadell, C.F.; García-Senz, J. & Hernaiz Huerta, P.P. 2007. Cainozoic larger foraminifers from Dominican Republic. *Boletín Geológico y Minero*, **118**:359–384.

Serra-Kiel, J.S.; Gallardo-Garcia, A.; Razin, P.; Robinet, J.; Roger, J.; Grelaud, C.; Leroy, S. & Robin, C. 2016. Middle Eocene–Early Miocene larger foraminifera from Dhofar (Oman) and Socotra Island (Yemen). *Arabian Journal of Geosciences*, **9**:344. *doi:10.1007/s12517-015-2243-3*

Serra-Kiel, J.S. *et al.* 1998. Larger foraminiferal biostratigraphy of the Tethyan Palaeocene and Eocene. *Bulletin de la Societe Géologique de France*, **169**:281–299.

Sirel, E. 2003. Foraminiferal description and biostratigraphy of the Bartonian, Priabonian, and Oligocene shallow-water sediments of southern and eastern Turkey. *Revue de Paléobiologie*, **22**:269–339.

Sirel, E. 2009. Reference sections and key localities of the Paleocene stages and their very shallow/shallow-water three new benthic foraminifera in Turkey. *Revue de Paléobiologie*, **28**:413–435.

Stöcklin, J. 1968. Structural History and Tectonics of Iran: A Review. *AAPG Bulletin*, **52**:1229–1258.

Stöcklin, J. 1977. Structural correlation of the alpine ranges between Iran and Central Asia. *Mémoires de la Société Géologique de France*, **8**:333–353.

Stöcklin, J. & Setudehnia, A. 1991. *Stratigraphic Lexicon of Iran*. Geological Survey of Iran, vol. 18, 376 p.

Stoneley, R. 1981. The geology of the Kuh–e Dalneshin area of Southern Iran, and its bearing on the evolution of Southern Tethys. *Journal of the Geological Society*, **138**:509–526.

Toumarkine, M. & Luterbacher, H.P. 1985. Paleocene and Eocene Planktic Foraminifera. *In*: H.M. Bolli; J.B. Saunders & K. Perch-Nielsen (eds.) *Plankton Stratigraphy*, Cambridge University Press, p. 87–154.

Wade, B.S.; Pearson, P.N.; Berggren, W.A. & Palike, H. 2011. Review and revision of Cenozoic tropical planktonic foraminiferal biostratigraphy and calibration to the geomagnetic polarity and astronomical time scale. *Earth-Science Reviews*, **104**:111–142. *doi:10.1016/j.earscirev.2010.09.003*

Wernli, R.; Morend, D. & Piguet, B. 1997. Les foraminifères planctoniques en sections de l'Eocène et de l'Oligocène des Grès de Samoëns (Ultra-helvétique du massif de Platé, Haute-Savoie, France). *Eclogae Geologicae Helvetiae*, **90**:581–590.

Zahedi, M. & Rahmati Ilkhechi, M. 2006. *Explanation of Geology of Shahrekord quadrangle, 1: 250000*. Geological Survey of Iran, 194 p.

Received in 11 February, 2022; accepted in 02 August, 2022.